Learning How to Smile: Can Rational Learning Explain the Predictable Dynamics in the Implied Volatility Surface?

Alejandro Bernales and Massimo Guidolin*

Abstract

We develop a general equilibrium asset pricing model under incomplete information and rational learning to explain the yet unexplained predictability of option prices. In our model, the fundamental dividend growth rate is unknown and subject to breaks, with time periods between breaks that follow a memory-less stochastic process. Immediately after a break there is insufficient information to price option contracts accurately. However, as new information arrives a representative Bayesian agent recursively learns about the parameters of the process followed by fundamentals. We show that learning makes beliefs time-varying in ways that induce large and dynamic risk premia in option prices and their implied volatilities. In addition, we find that learning generates different effects across option contracts with different strike prices and maturities. This induces realistic movements in the volatility surface implicit in option prices.

Keywords: option pricing, rational learning, Bayesian updating, implied volatility, predictability.

* Alejandro Bernales is at la Banque de France (Financial Economics Research Service, DGEI-DEMFI-RECFIN), e-mail: alejandro.bernales@banque-france.fr. Massimo Guidolin is at IGIER, Bocconi University, and CAIR, Manchester Business School, e-mail: massimo.guidolin@unibocconi.it. The authors thank Michael Brennan, Christian Hellwig, Jean-Stéphane Mésonnier, Gaetano Gaballo, Alex Taylor, Stuart Hyde, and Mario Cerrato for their comments on earlier versions of this paper. Additionally, we would like to thank seminar/session participants at Banque de France, Central Bank of Chile, the 2012 Financial Management Association Conference in Atlanta, the 2012 French Economic Association Conference in Paris, the 2013 Market Microstructure and Nonlinear Dynamics workshop in Evry, and Rouen Business School. The authors are grateful for the computational resources proportioned by the computing grids MACE and MAN2 at the University of Manchester and especially for the useful help from Simon Hood and Michael Croucher in running algorithms in the grids (MACE is part of the Mechanical, Aerospace & Civil Engineering School, while MAN2 is part of the British North Western Grid).

Learning How to Smile: Can Rational Learning Explain the Predictable Dynamics in the Implied Volatility Surface?

Abstract

We develop a general equilibrium asset pricing model under incomplete information and rational learning to explain the yet unexplained predictability of option prices. In our model, the fundamental dividend growth rate is unknown and subject to breaks, with time periods between breaks that follow a memory-less stochastic process. Immediately after a break there is insufficient information to price option contracts accurately. However, as new information arrives a representative Bayesian agent recursively learns about the parameters of the process followed by fundamentals. We show that learning makes beliefs time-varying in ways that induce large and dynamic risk premia in option prices and their implied volatilities. In addition, we find that learning generates different effects across option contracts with different strike prices and maturities. This induces realistic movements in the volatility surface implicit in option prices.

Keywords: option pricing, rational learning, Bayesian updating, implied volatility, predictability.

1 Introduction

Contrary to the constant volatility assumption of Black and Scholes' (1973) model (henceforth, BS), the volatilities implicit in option contracts change over time. Moreover, it is well known that at least from a statistical perspective, strong predictability patterns exist in implied volatilities and option prices (see, e.g., Harvey and Whaley, 1992; Heston and Nandi, 2000; Gonçalves and Guidolin, 2006; Konstantinidi *et al*., 2008; Christoffersen *et al.*, 2009). Additionally, and also in sharp contrast with BS assumptions and pricing results, the volatilities implicit in option contracts written on the same underlying asset systematically differ across strike prices and expiration dates. These cross-sectional differences in implied volatilities are known as the implied volatility surface, henceforth IVS (see, e.g., Rubinstein, 1994; Dumas *et al.*, 1998; Das and Sundaram, 1999). Historically, while BS constant volatility assumption was initially believed to characterize market option prices reasonably well (see, e.g., Rubinstein, 1985), since the 1987 market crash, data have been found to be inconsistent with BS because of the presence of persistent implied volatility smiles/skews and term structures. Furthermore, and similarly to the behaviour of the implied volatility of a single option contract, there is evidence of predictable dynamics in the shape characteristics of the *IVS* (see, e.g., Gonçalves and Guidolin, 2006; Chalamandaris and Tsekrekos, 2010).

In spite of this widespread and compelling evidence of dynamics in the volatilities implicit in traded options, there has been a limited effort in the financial economics literature aimed at developing equilibrium pricing models that may generate from first principles (i.e., from simple and generally accepted assumptions concerning preferences and the stochastic process of fundamentals driving asset prices) such ubiquitous patterns of dynamic predictability in the IVS.[1] The main goal of our research is to fill this gap by developing a rather standard and yet novel and powerful equilibrium model in which the investors' rational learning process explains the predictable dynamics in option prices and in the corresponding IVS.

We develop a discrete-time endowment, Lucas-type economy in which a representative agent trades in a risk-free, one-period bond, in a stock, and in a set of option contracts with different strike prices and expiration dates. The stock pays out an infinite stream of real dividends which

[1] A handful of exceptions are however discussed below, also to isolate our distinctive contribution. There is of course a growing literature that has proposed econometric models for the IVS and tested whether these may support profitable, out-of-sample trading strategies, see e.g., Dumas *et al.* (1998), Gonçalves and Guidolin (2006), Fengler (2009), Kim and Lee (2013).

evolve according to a geometric random walk; however, the mean dividend growth rate, g_t, is subject to infrequent (and always observable) breaks where the time periods between breaks follow a memory-less stochastic process. In the case in which a break takes place, the new mean dividend growth rate is drawn from a continuous univariate density $g_{t+1} \sim G(\cdot)$ defined on the support $[g_d, g_u]$. Even though breaks are observable, g_t is unknown to the agent, who recursively obtains incomplete information about the mean growth rate by observing independently distributed but noisy daily dividend realizations. The agent efficiently uses these signals following a rational Bayesian updating (learning) process.[2] Immediately after a break, historical information is scarce and this makes signals potentially unreliable; as a result, drastic revisions of beliefs concerning the new post-break value of g_t become likely. As long as no new stochastic breaks occur (given their infrequent nature, this is likely), these initial large updates in beliefs gradually decline as the agent endogenously learns as new information arrives. Nevertheless, learning never disappears completely, even asymptotically, because its strength is destined to be revived after a new break hits the mean growth rate. Therefore, breaks in the mean growth rate induce two main effects on all assets. First, breaks in g_t impact the stochastic evolution of future dividends, affecting the pricing of all securities directly. Second, breaks modify the quantity and reliability of the information that the agent has access to regarding the mean dividend growth rate g_t and hence breaks change the speed and intensity with which the investor updates her beliefs. Moreover, given that the learning process produces dynamic effects in beliefs, this process of recursive belief adjustments is responsible for a corresponding, highly nonlinear dynamics in options prices and in the associated IVS.

Financial markets and the economy are subject to continuous changes that force investors to an ever progressing process of learning on the fundamentals. There is a vast literature reporting breaks in economic fundamentals, such as in the parameters of the dividend process and in the real GDP growth (e.g., Bai *et al.*, 1998; Timmermann, 2001; Granger and Hyung, 2004). Breaks in fundamentals could be due to permanent technological innovations, shifts in tax codes, shifts in monetary policy, or shifts in stock market participation, among other possibilities. However, breaks in economic fundamentals will require that agents optimally

[2] Because under rather general condition that are satisfied under our simple set-up with observable breaks, it can be shown that the application of Bayes rule to the learning problem is equivalent to rational updating (see, e.g., Bray and Kreps, 1987; Guidolin and Timmermann, 2007), in the following we shall write about Bayesian and rational learning as if the two terms are identical.

follow a rational belief updating mechanism as they need to understand the resulting, new market conditions. Therefore, our study proposes a simple and yet powerful model—in terms of its far-reaching implications for our understanding of the dynamic process followed by option prices and the related IVS)—that purely relies on the interaction between rational learning and infrequent structural breaks to explain a number of so far frequently documented but not yet well understood features of the way options are priced.

Through an extensive set of simulations that price options with strikes and maturities determined according to the same (listing and delisting) rules that are actually followed in established option markets, we show that Bayesian learning induces dynamic patterns in option prices and implied volatilities (henceforth, IVs) that are consistent with what is reported by the empirical literature. We find that learning produces different dynamics in the implied volatilities across strike prices and time-to-maturities and thus induces movements in the shape of the IVS. We also show that learning induces serial correlation and volatility clustering in implied volatilities as well as in (measures of) the slope and curvature of the IVS.[3] We compare the results of our simulations, using a range of IVS predictability measures, with option market data concerning S&P 500 index options and a number of equity options traded in the U.S. to show that our incomplete information model generates to a large extent the same predictable features described by traded option prices.

The closest papers related to ours are David and Veronesi (2009), Guidolin and Timmermann (2003), and Shaliastovich (2008). These studies explore the effects of learning on option prices, measured at a certain point in time (i.e., they mostly perform a static analyses), to explain the different implied volatilities across strike prices and maturity dates which define the IVS. These studies show that learning induces asymmetric slopes and curvatures in the IVS, which is a result of course also obtained by our model. However, our focus is prominently on providing a rational, asset pricing-based explanations for the movements over time and the predictability in the IVS, besides calibrating the shape of the IVS itself. For instance, and differently from these earlier papers, our focus is devoted to calibrating and explaining autocorrelations in implied volatilities, the volatility clustering of implied volatilities, or the predictability patterns in slopes and curvatures of the IVS. In particular, David and Veronesi (2009) introduce a

[3] Predictability patterns in the level, slope, and curvature of the IVS have been already reported in empirical studies using S&P 500 index options (e.g., Gonçalves and Guidolin, 2006) as well as individual equity options (e.g., Bernales and Guidolin, 2012).

continuous-time model in which the dividend drift follows a two-state regime switching process. In their model, investors' uncertainty about the current state of the economy induces cross-sectional implied volatility skews and systematic shapes in the term-structure of the IVS. In our paper, we work in discrete time and with rare, infrequent breaks, not regimes, while our focus is distinctively on the IVS and its dynamic features.[4] Guidolin and Timmermann (2003) present a discrete-time equilibrium model in which the mean dividend growth rate evolves between two states in a binomial lattice with an unknown but recursively updated state probability. However, in Guidolin and Timmermann's work, learning effects vanish asymptotically as time deterministically flows because investors eventually achieve complete knowledge of the unknown state probability.[5] Moreover, our model is more general than a simple binomial lattice and, although less theoretical results can be precisely documented, its calibrated versions give more realistic predictions than in Guidolin and Timmermann's. Shaliastovich (2008) introduce a discrete-time long-run risk type model in which the unobservable consumption growth rate has to be learned via a "recency"-biased updating procedure. In his paper, expected consumption growth and its uncertainty are time-varying, while uncertainty is subject to jumps. Compared to his paper, we use a simpler model with no long run risks or jumps, but restrict the investor to rationally learn about the mean growth rate since the most recent structural break.

There are a few more papers that are somewhat related to our research, although they do not specifically investigate the effects of learning on predictable option IV dynamics. Our research has links to studies that examine structural breaks in economic fundamentals in relation to the effects of learning on stock prices and their return process (e.g., Timmermann, 2001; Pastor and Stambaugh, 2001). Lettau and Van Nieuwerburgh (2008) have documented that the stock return predictability puzzle can be explained by breaks in economic fundamentals. They show that in-sample financial ratios and future returns are significantly related; however, in real time this relationship cannot be exploited due to occurrence of infrequent breaks. Lettau and Van Nieuwerburgh also report that return predictability is mainly affected by the uncertainty

[4] In this sense, the most closely related papers are Timmermann (2001) and Guidolin (2006), where infrequent breaks are modelled and empirically estimated, but the goal is simply to explain the empirical features of the realized distribution of stock returns, such as the equity premium, volatility clustering, excess kurtosis, etc.

[5] Although Guidolin and Timmermann (2003) perform a dynamic analysis, they only examine the weekly fit of their model over time. Therefore, they do not study specifically whether their model may generate predictable dynamics in option prices and the associated *IVS*.

induced in the estimation of the new fundamental value after breaks, whereas the uncertainty generated by the detection of breaking dates is less critical. Ederington and Lee (1996) and Beber and Brandt (2006, 2009) show that macroeconomic events or news at both expected and unexpected times increase implied volatilities, while implied volatilities decline when uncertainty is resolved. Donders *et al.* (2000), Dubinsky and Johannes (2006), and Ni *et al.* (2008) present similar results to Ederington and Lee and Beber and Brandt's, although they mostly focus on the effects of earnings announcement dates on implied volatilities.

The rest of the paper is organized as follows. Section 2 presents the model, and section 3 describes the simulations and results. Specific subsections document at first the nature of our qualitative results, i.e., the fact that a model such as the one proposed "can do the job" requested of it, and then perform a quantitative calibration aimed at showing that the framework may re-produce standard econometric evidence on the predictability of the IVS. Concluding remarks appear in section 4.

2 The Model

2.1 Option Pricing under Breaks and Complete Information

We consider a representative agent discrete-time endowment economy as in Lucas (1978). This economy contains three types of assets: a one-period zero-coupon default free bond, B_t, in zero net supply; a stock with net supply normalized at one, S_t; and a set of redundant call option contracts, $Call_t(K,\tau)$, which are European-style with underlying asset priced at S_t, strike price K, and time-to-maturity τ. The stock pays out an infinite stream of real dividends, D_t; however the mean (continuously compounded) dividend growth rate, $g_t \equiv \ln(D_t/D_{t-1})$, is subject to unpredictable breaks. The time periods between breaks follow a memory-less geometric process parameterized by π; and thus the number of breaks in a given period follows a Binomial distribution.[6] We assume that when a break occurs, the new mean dividend growth rate is obtained from a continuous univariate density, $g_{t+1} \sim G(\cdot)$, defined on the support $[g_d, g_u]$. In addition, net of the break dynamics, dividends evolve according to a geometric random walk process with constant volatility σ and drift μ_{t+1},

[6] Shaliastovich (2008) uses a continuous-time Poisson process in his discrete-time learning model to describe jumps in the uncertainty over time, and thus time periods between jumps follow a memory-less exponential process which is also in continuous-time. This kind of set-up is common in the literature. However, we prefer to be consistent with our discrete-time model; and thus we use a discretized version of the Poisson and exponential processes which are the Binomial and the memory-less geometric processes, respectively.

$$\ln\left(\frac{D_{t+1}}{D_t}\right) = \mu_{t+1} + \sigma\varepsilon_{t+1} \tag{1}$$

in which the innovation term, ε_{t+1}, is homoscedastic and serially uncorrelated; however, μ_{t+1} changes over time since it is related to g_{t+1} by $1 + g_{t+1} = \exp(\mu_{t+1} + \sigma^2/2)$. [7]

We assume a perfect, frictionless, and complete capital market: there are no taxes, no transaction costs, unlimited short sales possibilities, perfect liquidity, and no borrowing and lending constraints. As discussed in Brennan and Cao (1996), it is market completeness that makes options redundant assets. The representative agent has preferences described by a standard, power utility function,

$$u(C_t) = \begin{cases} \dfrac{C_t^{1-\alpha} - 1}{1-\alpha} & \alpha \geq 0 \\ \ln C_t & \alpha = 1 \end{cases} \tag{2}$$

where C_t is real consumption and α corresponds to her constant coefficient of relative risk aversion (CRRA). We assume that dividends represent the unique source of income of this representative agent. As typical in a Lucas-type model, dividends are perishable and consumed when they are received at any time $t + k$ (i.e., $C_{t+k} = D_{t+k}$). Therefore the representative agent maximizes the discounted value of her expected stream of future utility choosing assets' holdings and subject to a standard budget constraint,

$$\max_{\{D_{t+k}, w^S_{t+k}, w^B_{t+k}\}} E_t\left[\sum_{k=0}^{\infty} \beta^k u(D_{t+k})\right] \tag{3}$$
$$\text{s.t.} \quad C_{t+k} + w^S_{t+k} S_{t+k} + w^B_{t+k} B_{t+k} \leq w^S_{t+k-1}(S_{t+k-1} + D_{t+k-1}) + w^B_{t+k-1}$$

where $\beta \equiv 1/(1+\rho)$, ρ is the subjective impatience rate, and w^S_{t+k} (w^B_{t+k}) are the shares of stocks (bonds) in her portfolio. Since call option contracts are redundant assets in zero endogenous net supply, option holdings do not affect the agent's optimization because they fail to appear in her budget constraint. Therefore, option holdings do not affect stock and bond

[7] We assume that σ is constant to obtain the simplest setting, in which only one parameter is to be learned, to analyse the impact of learning on the dynamics of option prices. This is consistent with earlier work by Timmermann (1996, 2001) who, with reference to equilibrium equity prices, has shown that the investors' learning regarding only the mean dividend growth rate is sufficient to induce excess volatility and volatility clustering in stock returns, even though the volatility of the dividend random walk process is constant.

prices. Consequently, Euler equations are obtained for the stock and bond by standard dynamic programming methods (see, e.g., Pliska, 1997):

$$S_t = \mathrm{E}_t\left[\beta\left(\frac{D_{t+1}}{D_t}\right)^{-\alpha}(S_{t+1}+D_{t+1})\right] \tag{4}$$

$$B_t = \mathrm{E}_t\left[\beta\left(\frac{D_{t+1}}{D_t}\right)^{-\alpha}\right] \tag{5}$$

where $Q_{t+1} = \beta(D_{t+1}/D_t)^{-\alpha}$ is the pricing kernel defined as the intertemporal marginal rate of substitution multiplied by the subjective discount factor.

In this section, we assume complete knowledge of the parameters appearing in the process for real dividends. This means that both μ_t and σ are known. Of course, μ_t remains time-varying so that knowledge of μ_t does not imply it is identical to μ_{t+1}. However, also the occurrence of breaks is assumed to be observable. Moreover, under complete information (CI), we assume that the distribution from which log-growth rates are drawn, $g_{t+1}\sim G(\cdot)$ with support $[g_d, g_u]$, is also known to the representative investor. Under these simplifying restrictions, although the Euler conditions in (4) and (5) appear to be standard in the literature, solving them as difference equations in the presence of infrequent breaks but complete information yields non-trivial expressions for equilibrium stock and bonds prices, presented in Proposition 1.

PROPOSITION 1 (Complete Information): *Assuming that the mean growth rate g_t is subject to breaks, and that when a break occurs (with probability π), the new mean dividend growth rate is drawn from a given univariate density $g_{t+1}\sim G(\cdot)$ with support $[g_d, g_u]$, where $1+\rho > (1+g_u)^{1-\alpha}$, then the stock and bond prices under complete information, S_t^{CI} and B_t^{CI}, are:*

$$\begin{aligned} S_t^{CI} &= \frac{D_t}{1+\rho-(1-\pi)(1+g_t)^{1-\alpha}}\left\{(1-\pi)(1+g_t)^{1-\alpha}+\pi\left(\frac{I_1+(1-\pi)I_2}{1-\pi I_3}\right)\right\} \\ &= D_t\Psi(g_t) \end{aligned} \tag{6}$$

where

$$I_1 = \int_{g_d}^{g_u}(1+g_{t+1})^{1-\alpha}dG(g_{t+1})$$

$$I_2 = \int_{g_d}^{g_u}\frac{(1+g_{t+1})^{2-2\alpha}}{1+\rho-(1-\pi)(1+g_{t+1})^{1-\alpha}}dG(g_{t+1})$$

$I_3 = \int_{g_d}^{g_u} \frac{(1+g_{t+1})^{1-\alpha}}{1+\rho-(1-\pi)(1+g_{t+1})^{1-\alpha}} dG(g_{t+1})$;

moreover

$$B_t^{CI} = \frac{1}{(1+\rho)} \left\{ (1-\pi)(1+g_t)^{-\alpha} + \pi \int_{g_d}^{g_u} (1+g_{t+1})^{-\alpha} dG(g_{t+1}) \right\}, \tag{7}$$

in which the one-period risk-free interest rate is defined as $r_t^{CI} \equiv 1/B_t^{CI} - 1$.

Proof: See appendix A

Proposition 1 has a number of neat implications. The ex-dividend (real) stock prices are first order homogeneous in dividends and are affected by breaks in g_t. Consequently, the price-dividend ratio is time-varying and also conditional on g_t. This means that while in the absence of breaks (as in GT, 2003), the CI stock price is simply,

$$S_t^{CI,\pi=0} = \frac{(1+g_t)^{1-\alpha}}{1+\rho-(1-\pi)(1+g_t)^{1-\alpha}} D_t = \Psi^{\mathrm{CI}} D_t$$

where the price-dividend ratio (Ψ^{CI}) is constant over time, the possibility of breaks occurring makes by itself the stock price volatile, both through changes—albeit, infrequent—in the price-dividend ratio and in the plain level of real dividends. Note that in the logarithmic utility case, as it is well known (see e.g., Veronesi, 1999), when $\alpha = 1$, then

$$S_t^{CI,\alpha=1} = \frac{1+\pi\rho}{1+\rho-(1-\pi)} D_t \tag{8}$$

so that the price-dividend ratio is constant that also depends on π.

Similarly, the one-period zero-coupon bond changes over time due to shifts in g_t. The one-period zero-coupon bond price is given by the expected pricing kernel in the absence of breaks (when $\pi = 0$), $(1+g_t)^{-\alpha}/(1+\rho)$, multiplied by the probability of no breaks $(1 - \pi)$ plus the expected pricing kernel in the case of breaks, $\int_{g_d}^{g_u}(1+g_t)^{-\alpha} dG(g_t)/(1+\rho)$, multiplied by the probability of breaks, π. Additionally, the current expected forward price of a one-period zero-coupon bond in the very long-term is equal to the expected value of the pricing kernel in the

scenario of a break since the probability of having no shifts in the mean in the distant future is practically zero (i.e., $\lim_{s\to\infty} E_t[B_s^{CI}] = \int_{g_d}^{g_u}(1+g_t)^{-\alpha}dG(g_t)/(1+\rho)$).

Furthermore, pricing European call option contracts is straightforward under complete information. We assume that there are no arbitrage opportunities, and the agent makes portfolio choices considering asset menus that include stocks and bonds only. This derives from our earlier assumption that markets are complete, so that European options are redundant by construction. In the case of an economy without breaks (i.e. $\pi = 0$), no-arbitrage option prices can be computed as Black-Scholes (BS) prices deriving from equilibrium models in which the dividend fundamental process is stationary (see GT, 2003, and references and proofs therein).[8] However, Black-Scholes' formula fails to hold, even an approximation, when breaks in g_t are possible. Breaks make dividend yields and interest rates time-varying, thereby introducing non-stationarities in the dynamics process followed by the primitive assets that underlie the no-arbitrage of European options. For instance, an option contract should be now priced taking into account that there exists a probability $\pi > 0$ that g_t may affected by a structural, and possibly permanent change in any period before the options expiration date. Therefore, the correct discount factors to be applied—even under the risk-neutral measure that characterizes BS pricing—are path-dependent. Nevertheless, option contracts can be priced by a change of measure to the state-price density. Proposition 2 presents an expression for European call option prices based on this change of measure; Section 3 shows how the resulting expression may be solved using numerical methods.

PROPOSITION 2 (Complete Information): *Under complete information, the no-arbitrage price of European call contract written on the stock, with strike price K and time-to-maturity τ is:*

$$Call_t^{CI}(K,\tau) = \int_0^{\infty} \max\{S_{t+\tau}^{CI} - K, 0\}\,\tilde{p}_t(S_{t+\tau}^{CI})dS_{t+\tau}^{CI} \qquad (9)$$

where $S_{t+\tau}^{CI} = D_{t+\tau}\Psi(g_{t+\tau})$, $D_{t+\tau} = D_t \exp\left(\sqrt{\tau}\sigma\varepsilon_{t+\tau} - \tau\sigma^2/2\right)\prod_{i=0}^{z}(1+g_{t+h_i})^{h_i}$, $\varepsilon_{t+\tau}$ *is the innovation term of the dividend geometric random walk process in* (1) *distributed as a normal density* $\phi(\varepsilon_{t+\tau}|0,\sigma)$ *with mean zero and variance* σ, $z \leq \tau$ *is the number of breaks between* t *and* $t+\tau$, *a random variable drawn from a Binomial distribution* $\varphi(z|\tau,\pi)$ *with parameters* τ *and* π,

[8] Technically, this result obtains only in the continuous time limit. However, here we refer to a discretized Black-Scholes, fundamental-based formula that in fact goes back to the seminal paper by Rubinstein (1976).

$\{h_i\}_{i=0}^{z}$ are the time intervals between breaks, drawn from geometric distributions $\eta(h_i|\pi)$ in which $\tau = \sum_{i=0}^{z} h_i$. In addition, the new, future post-break growth rates $\{g_{t+h_i}\}_{i=1}^{z}$ are drawn from a univariate density $g_{t+h_{i-1}} \sim G(\cdot)$ with pdf $\varrho(\cdot)$ defined on the support $[g_d, g_u]$ where $g_{t+h_0} = g_t$ and $g_{t+\tau} = g_{t+h_z}$. Finally, the state price density is characterized as:

$$\tilde{p}_t(S_{t+\tau}^{CI}) = \beta^{\tau}\left(\frac{D_{t+\tau}}{D_t}\right)^{-\alpha} \phi(\varepsilon_{t+\tau}|0,\sigma)\varphi(z|\tau,\pi)\eta(h_0|\pi)\left(\eta(h_1|\pi)\varrho\left(g_{t+h_1}\right)\cdot \ldots \cdot \eta(h_z|\pi)\varrho\left(g_{t+h_z}\right)\right).$$

Proof: See appendix A

2.2 Option Pricing under Breaks and Incomplete Information with Bayesian Learning

In Section 2.1, the equations for pricing the bond, the stock (tree), and any cross-section of option contracts introduced in Propositions 1 and 2 were derived assuming that the agent knows the volatility parameter σ and especially, the true mean dividend growth rate at each point in time. However, these expressions are not valid when there is incomplete information in the economy and an investor needs to learn the unknown parameters driving the process of fundamentals. Suppose that g_t is unknown and the representative agent efficiently uses all available information to price the assets following a Bayesian updating procedure. Within each regime, as defined by the last occurrence of a break, the agent receives new, independent signals about the mean dividend growth on a daily basis, $\{D_i/D_{i-1}\}_{i=t-n+1}^{t}$, which are random and follow a lognormal distribution where n is the number of periods since the last break (see equation (1)). However, breaks are still assumed to consist of rarely occurring and rather visible events so that they are observable. The investor's learning therefore concern only the actual value of g_t following the most recent break. Although it would be possible to extend our set up to model the effects induced by any learning/estimation of breakpoint dates, the cost of this extension in terms of analytical complexity is remarkable, with a consequent loss of intuition for the results to be derived below. Moreover, assuming knowledge of the breakpoint dates does not appear to be completely unrealistic, as a number of recent econometric advances have shown that it is possible to perform real time tests monitoring breaks in the

mean function, attaining a considerable degree of accuracy, see e.g., Chu *et al*. (1996) and Leisch *et al*. (2000).[9]

The representative agent uses her prior beliefs while she recursively learns, incorporating the all the new information received. Therefore, as in Timmermann (2001), the expected value of any asset, $\lambda_t(g_t|\pi,\rho,\alpha,\sigma)$, given an agent's prior beliefs $\varrho(g_t)$ can be simply obtained from the following updating Bayesian rule

$$\mathrm{E}_{t,n}^{BL}[\lambda_t(g_t)|\mathbf{q}_t] = \frac{\int_{g_d}^{g_u} \lambda_t(g_t) L(g_t|\mathbf{q}_t)_n \varrho(g_t) dg_t}{\int_{g_d}^{g_u} L(g_t|\mathbf{q}_t)_n \varrho(g_t) dg_t} \tag{9}$$

where $L(g_t|\mathbf{q}_t)_n$ is the sample likelihood function, and the vector of signals is represented by $\mathbf{q}_t = [(D_t/D_{t-1}) \dots (D_{t-n+1}/D_{t-n})]$. The intuition behind equation (9) is simple. The agent does not know the new value of g_t after a break but she knows the distribution followed by g_t ($\varrho(g_t)$) and the distribution followed by the signal vector $\mathbf{q}_t$. Given this knowledge, the agent recursively updates her expectations about g_t and on the value of all assets that depend of g_t, $\lambda_t(g_t)$, as new signals are observed using Bayes' rule. After a break affecting the true but unknown value of g_t, the new value will only be gradually learned because of the contemporaneous presence of the random innovation in the random walk process followed by dividends, for a given growth time-varying parameter g_t. Therefore, in addition to the non-stationarities induced by the very presence of breaks in the process followed by the price of all assets, incomplete information and learning will generate incremental randomness in the value of stocks, bonds, and option prices.

In equation (9), instead of dealing with a complex sample likelihood function concerning log-normally distributed data, it is convenient to re-write Bayes' rule taking μ_t as the unknown parameter without loss of generality, because $1 + g_t = \exp(\mu_t + \sigma^2/2)$. The main advantage of parameterizing (9) as a function of μ_t is that the observable signals, $\{\ln(D_i/D_{i-1})\}_{i=t-n+1}^{t}$, will now follow a normal density, so that equation (9) can be written as:

[9] Additionally, Lettau and Van Nieuwerburgh (2008) have shown that the uncertainty generated by the detection of breakpoint dates in the process of economic fundamentals is not critical to explain stock returns anomalies. Lettau and Van Nieuwerburgh (2008) show that the main source of uncertainty is caused by the estimation of the magnitude of the new parameters in the aftermath of the break dates, similarly to our modelling approach.

$$\mathrm{E}_{t,n}^{BL}[\lambda_t(\mu_t)|\boldsymbol{\xi}_t] = \frac{\int_{\mu_d}^{\mu_u} \lambda_t(\mu_t) L(\mu_t|\boldsymbol{\xi}_t)_n f(\mu_t) d\mu_t}{\int_{\mu_d}^{\mu_u} L(\mu_t|\boldsymbol{\xi}_t)_n f(\mu_t) d\mu_t} \tag{10}$$

with

$$L(\mu_t|\boldsymbol{\xi}_t)_n = \frac{1}{\sqrt{2\pi\sigma^2/n}} \exp\left[\frac{-\left(\bar{\xi}_t - \mu_t\right)^2}{2\sigma^2/n}\right] \tag{11}$$

in which $\boldsymbol{\xi}_t = [\ln(D_t/D_{t-1}) \ldots \ln(D_{t-n+1}/D_{t-n})]$, and $\bar{\xi}_t = (1/n)\sum_{i=t-n+1}^{t} \xi_i$ is the sample mean. At this point, building on equations (10) and (11), it is possible to derive results for the price of assets in the presence of infrequent breaks and under incomplete information with learning. Interestingly, these use the closed-form expressions under complete information already derived in Propositions 1 and 2.

PROPOSITION 3 (Bayesian Learning): *Assuming incomplete information and learning, the stock and bond prices are given by:*

$$S_t^{BL} = \frac{\int_{\mu_d}^{\mu_u} S_t^{CI} L(\mu_t|\boldsymbol{\xi}_t)_n f(\mu_t) d\mu_t}{\int_{\mu_d}^{\mu_u} L(\mu_t|\boldsymbol{\xi}_t)_n f(\mu_t) d\mu_t} \tag{12}$$

and

$$B_t^{BL} = \frac{\int_{\mu_d}^{\mu_u} B_t^{CI} L(\mu_t|\boldsymbol{\xi}_t)_n f(\mu_t) d\mu_t}{\int_{\mu_d}^{\mu_u} L(\mu_t|\boldsymbol{\xi}_t)_n f(\mu_t) d\mu_t} \tag{13}$$

where S_t^{CI} and B_t^{CI} are the stock and bond price expressions under breaks and complete information defined in Proposition 1.

PROPOSITION 2 (Bayesian Learning): *Under incomplete information and learning, the prices of European call options written on the stock, with strike price K, and time-to-maturity $\tau = T - t$ are:*

$$\begin{aligned} &Call_t^{BL}(K,\tau) \\ &= \frac{\int_{\mu_d}^{\mu_u} \left\{\int_0^{\infty} \max\{S_{t+\tau}^{CI} - K, 0\} \tilde{p}_t(S_{t+\tau}^{CI}) dS_{t+\tau}^{CI}\right\} L(\mu_{t+\tau}|\boldsymbol{\xi}_{t+\tau})_{n_{t+\tau}} f(\mu_{t+\tau}) d\mu_{t+\tau}}{\int_{\mu_d}^{\mu_u} L(\mu_{t+\tau}|\boldsymbol{\xi}_{t+\tau})_{n_{t+\tau}} f(\mu_{t+\tau}) d\mu_{t+\tau}} \end{aligned} \tag{14}$$

where $S_{t+\tau}^{CI} = D_{t+\tau}\Psi(g_{t+\tau})$, $g_{t+\tau} = \exp(\mu_{t+\tau} + \sigma^2/2) - 1$, *dividends on expiration date follow* $D_{t+\tau} = D_t \exp\left(\sqrt{\tau}\sigma\varepsilon_{t+\tau} - \tau\sigma^2/2\right)\prod_{i=0}^{z}(1 + g_{t+h_i})^{h_i}$, $\varepsilon_{t+\tau}$, $z \leq \tau$, $\{h_i\}_{i=0}^{z}$, $\{g_{t+h_i}\}_{i=1}^{z}$, *and* $\tilde{p}_t(S_{t+\tau}^{CI})$ *are as in Propostion 1. In addition,* $n_{t+\tau}$ *is the number of dividend signals since the last break.*[10]

The simplicity of the Bayesian updating procedure underlying Propositions 1 and 2 is useful to our understanding of the effects of learning on asset prices. In this perspective, we start by analyzing two special cases that are illustrative of the mechanics of the effects of Rational learning. First, suppose that the probability of a break is very large, $\pi \to 1$. This implies that the agent faces very frequent breaks, at the same frequency as calendar time (say, daily). In this case, learning has no effects because g_t changes in correspondence to all *t*s, so that "there is no time for the investor to learn". In this case, the expressions (12)-(14) simplify to (6)-(8) under the restriction that $\pi = 1$. Second, when $\pi = 0$ learning vanishes as $t \to \infty$, as in GT (2003). In this case the agent should have sufficient information after a long period to calculate accurate estimates for g_t and asset prices; and thus the effects of learning will disappear asymptotically. In this case, the expressions (12)-(14) converge to (6)-(8) under the restriction that $\pi = 0$.

In general, Propositions 1 and 2 show that after a break, substantial revisions in agents' expectations may occur that strongly affect asset prices. Immediately after breaks, the agent does not have enough historical information to obtain reliable estimates. Therefore, her portfolio choices and, in equilibrium, asset prices will reflect an initially intense period of learning that generates important changes in prices as a result of belief revisions. As we shall document in Section 2, such revisions and non-stationarities in the process of asset prices are responsible for inducing sizeable premia in the valuation process of all assets and particularly in option prices and in their implicit volatilities. However, these large revisions in beliefs progressively abate over time as more information is received and learned. This updating process of agents' beliefs, which is caused by recursive information acquisition, will induce rich patterns of predictable dynamics in option prices and implied.

[10] Note that $n_{t+\tau} \neq n + \tau$ since there are chances of breaks occurring between t and $t + \tau$; therefore $n_{t+\tau}$ is also a random variable, where $n_{t+\tau} \leq n + \tau$.

3 Simulation Results: Making Sense of the Econometric Evidence

3.1 The research design

The main goal of our research is to provide an understanding of whether and how a Bayesian learning scheme applied to processes subject to infrequent breaks, may explain a number of stylized facts concerning the pricing of European index options. We perform such an investigation also assessing the implications of alternative assumptions concerning learning dynamics, i.e., the features of the way investors update their expectations over time. Following the same arguments as Timmermann (1993, 1996, 2001), Veronesi (1999, 2000), Guidolin (2006), and Veronesi and David (2009), who all evaluate how the learning process affects the properties of stock returns by performing extensive sets of simulations, we use a quantitative Monte Carlo approach. In fact, all the papers cited above argue that learning influences the pricing function of all assets in a highly nonlinear way that would be poorly approximated by any attempts at log-linearization, so that simulations are necessary to understand the wide scope of outcomes that learning may induce.[11] Moreover, the use of simulations allows us to modify parameter configurations and observe the impact of learning in multiple environments.

As a first step in our Monte Carlo experiments, we reproduce the CBOE rules that generate option contract series made available for trading over time, in terms of strike price intervals, expiration dates, and listing and delisting policies. In previous studies (e.g., Duan and Simonato, 2001; Yan, 2011), options data have been simulated assuming constant moneyness and time-to-maturity for a specific option contract (for instance, exactly 30-day to expiry contracts with a moneyness exactly equal to one).[12] Clearly, on the one hand, the moneyness ratio changes constantly because strike prices are fixed by option exchanges while stock prices vary over time. On the other hand, the time-to-maturity decreases gradually since expiration dates are also fixed. Therefore, the assumption of regular and invariable features of the traded option contracts in a simulation exercise is not consistent with actual options data. Because our stated goal is to investigate whether Rational learning may re-produce a range of small-sample results generated from standard econometric tests applied to actual data, to generate a cross-sectional

[11] Kleidon (1986) shows that the use of standard tests to evaluate an equilibrium model using a single economy represented by market data may lead to inaccurate conclusions. He emphasizes that asset prices in equilibrium are calculated based on agents' expectations about future events across multiple and different economies. Instead, Kleidon proposes the use of multiple realizations by simulation techniques.

[12] We define moneyness as $Mon \equiv K/S$, where K and S are the strike and the underlying stock prices, respectively.

(across strikes and maturities) time-series panel of option prices in a realistic way plays a crucial role in case the null hypothesis of learning not being fundamentally responsible for the reported stylized facts were not to be rejected.[13] Instead, to increase the realism as well as the reliability of our results, we follow the detailed rules of the CBOE.

In particular, first, we use the same trading dates that were effectively listed over the 12-year sample 1996 - 2007, thus accounting for holidays and unexpected events in which the market was closed.[14] Second, we fix expiration dates for option contracts in the same way as the CBOE has been doing between 1996 and 2007. Therefore, for contracts to be offered in a given month, the expiration dates are set to coincide with the three subsequent months followed by three additional long-term maturities aligned on the March quarterly cycle (i.e., March, June, September, and December). In addition, expiration dates fall in correspondence of the Saturday after the third Friday of each expiration month. Third, strike price intervals are set around the underlying asset price; contracts with expiration dates in the three near-term months are spaced at 5-point intervals around the underlying index price as of the day in which contracts are offered, while contracts with long-term expirations are spaced at 25-point intervals.

Throughout this paper, we calculate implied volatilities (IVs) by numerically inverting the Black-Scholes (1973) model which is consistent with both previous academic studies and investor practice, where IVs are estimated using BS model even though it is well-understood that BS assumptions are violated by market data. Obviously, as already commented in Section 2, our model departs from BS because of the richer dynamics of the process of fundamentals, as well as because of the fact that index options written on the market are priced off fundamentals in complete markets, as in GT (2003).[15] Moreover, the well known predictability patterns in both IVs as well as in the shapes of the IVS, which we want to explain through our learning model, have been always reported and discussed with reference to implicit volatilities

[13] This means that we want to minimize the chances of Bayesian learning explaining option pricing stylized features and puzzles, but this hypothesis being rejected because prices are simulated following over-simplistic rules that make simulated results not perfectly comparable to the ones obtained from the data, that are instead generated following CBOE rules.

[14] However, for simplicity such infrequent and unexpected events (e.g., September 11, 2001) are not simulated and are held fixed throughout all simulation trials. Note that most of the existing literature has completely ignored the effects of such rare occurrences on econometric tests.

[15] Note that this claim is already true under complete information provided that $\pi > 0$. Of course, this is all the more correct under incomplete information, because of the effects of Bayesian learning and independently of whether $\pi > 0$ or not. However, when $\pi = 0$, note that the no-arbitrage option prices asymptotically converge to BS/Rubinstein prices as $t \to \infty$.

calculated with under BS model (see, among others, Harvey and Whaley, 1992; Gonçalves and Guidolin, 2006; Konstantinidi *et al*., 2008; Chalamandaris and Tsekrekos, 2010). In this respect, one may see the (probably misspecified) use of BS to compute implicit IVs as a "wash out": in the same way in which market data that are not generated from BS assumptions are transformed into BS IVs, simulated prices computed under alternative assumptions on the mechanism of expectation formation are transformed into IVs using the same, commonly used device, Black-Scholes, to make any comparisons possible.

3.2 Calibration

We assume the following parameter values to be held constant in the simulations that follow. In a few cases, especially as far preferences are concerned, we produce, tabulate and discuss results across a range of parameters to emphasize that these are hardly relevant—unless otherwise noted—to the general tone of our qualitative findings. The subjective rate of impatience, ρ, is set to equal either 0.713% or 0.767% (on a monthly basis). Using methods similar to GT (2003) and Guidolin (2006) we verify that on average, over our 1996-2007 sample path and using the parameters that follow, under incomplete information and Bayesian learning these parametric choices imply annualized equilibrium short-term rates that appear to be realistic with reference to the long-run properties of the U.S. financial market. We also assume that when ρ = 0.713% (ρ = 0.767%) the new mean dividend growth rate after breaks is extracted from a uniform distribution with upper and lower boundaries of $g_u = 8.8\%$ ($g_u = 9.5\%$) and $g_d = -1.5\%$ ($g_d = -5.0\%$), expressed in annualized terms. As a result, one can verify that $1 + \rho > (1 + g_u)^{1-\alpha}$ for all the values of CRRA employed in this paper (see below).[16] Proposition 1 shows that such a condition guarantees the existence of an equilibrium pricing function; because Proposition 3 relies on the same assumptions made in Proposition 1 under the case of complete information, this inequality is also sufficient for existence when learning occurs. The dividend process volatility, σ, is also set at two alternative values, 5% and 30% (on annual basis), to span a range of possibilities. Of course, 5% is consistent with the typical parameterizations for the process followed by real dividends in the U.S. (see e.g.,

[16] Therefore, and given that the new mean dividend growth rate after breaks is extracted from a uniform distribution with probability density function $f(g_t) = 1/(g_u - g_d)$, in corollary 1 and corollary 2 the dividend drift has as probability density function: $f(\mu_t) = \exp(\mu_t + \sigma^2/2)/(g_u - g_d)$, where $\mu_d = \ln(1 + g_d) - \sigma^2/2$ and $\mu_u = \ln(1 + g_u) - \sigma^2/2$.

Timmermann, 2001; GT, 2003). 30% represents instead a high-volatility case in which investors may be learning directly from past stock market returns, more than from the process of fundamentals itself.[17] Finally, as far as the CRRA coefficient α is concerned, we use $\alpha = 0.2$, $\alpha = 0.5$, and $\alpha = 5$. Levels of α below 1 are both consistent with the evidence in the data of a relatively high (certainly in excess of 2) intertemporal elasticity of substitution in consumption; because under power utility, such an intertemporal elasticity of substitution is simply the inverse of α, $\alpha < 1$ appears sensible. Moreover, evidence in Timmermann (2001) and Guidolin (2006) has shown that under Rational learning, provided an equilibrium exists, for $\alpha < 1$ the equity premium appears to be increasing in α as α declines towards zero (see also David, 2008), while the riskless short term rate declines (as it is customary in Lucas tree models). However, also because this level of the CRRA is commonly perceived as "acceptable" (even though it is inconsistent with commonly estimated intertemporal elasticity of substitution coefficients), we also entertain the case of $\alpha = 5$.

We use the recursive, real time monitoring breakpoint test introduced by Chu *et al.* (1996) to estimate a probability of breaks, π, affecting the mean real dividend growth rate. In Appendix B, we describe the model introduced by Chu *et al.* (1996) and the breaks detected by the application of their method to series of S&P 500 dividends over a 1996 – 2007 sample of daily data, which are also which are de-seasonalized and adjusted by the consumer price index to obtain real dividends. We find eight breaks in the 3,012 days of the 12-year sample analyzed in this paper. Therefore we set π at 0.00301 per day (0.667 on an annual basis). In essence, real dividend data confirm that breaks are indeed possible on a daily frequency, but only with a negligible probability of less than 1% per day; equivalently, the absence of breaks is expected to last on average for 333 days in a row, well in excess of one year.

As mentioned above, we simulate multiple scenarios depending on three assumptions about the representative agent's expectations: (A) an economy without breaks;[18] (B) an economy with breaks and complete information; and (C) an economy with breaks and incomplete

[17] In this paper we care for also entertaining the case of $\sigma = 30\%$ per year as in this case learning may only occur very slowly between structural breaks, as any signals concerning the drift of fundamentals is confounded by the high variability of diffusive shocks that hit them.

[18] In this case, it is irrelevant to specify whether information is complete or must be learned: also under Bayesian learning, if we were to simulate such an economy for a period of 12 years, we would obtain that by the end of the exercise, such an economy would behave in the same way as a complete information one. Therefore we simply assume that information is complete.

information, under Bayesian learning. In case (A) (when g is constant), we calculate stock and bond prices assuming that $\pi = 0$ using equations (6) and (7), respectively. In this case, European option prices are obtained from BS model in which the dividend yield is $\delta^{BS} = (1 + \rho - (1 + g_t)^{1-\alpha})/(1 + g_t)^{1-\alpha}$, see GT (2003) for a proof. In scenario (B) of an economy with breaks and complete information, stock and bond prices are calculated from (6) and (7) assuming $\pi = 0.00301$. In addition, European call prices are calculated using equation (8) where the main integral is solved by Monte Carlo methods, on the basis of 20,000 independent paths from the stochastic process described in Proposition 2. In scenario (C), the case of breaks and incomplete information with learning, stock and bond prices are obtained from (12) and (13) with $\pi = 0.00301$, while option prices from equation (14), using again Monte Carlo methods.[19]

Under each of the three alternative scenarios and for each possible combination of parameters—these are 12, from two values for ρ, two for σ, and three for the CRRA coefficient α—we generate 2,000 simulations. On each simulated path, we produce 12 years of daily real dividends (3,018 days) which represent the observable signals received by the investor and used to learn about g_t. The simulations are generated by the two-step subordinated stochastic processes described in equation (1). This means that in the absence of breaks (for a constant g), we simulate time series of 12 years of daily dividends using a geometric random walk process. Additionally, we induce stochastic breaks in g_t on each time step of each simulated path (hence, we generate breaks in μ_t) according to the assumed geometric process parameterized by π. For instance, in the case in which a break occurs at time $t = m$, we obtain a new value for g_m drawn from a uniform distribution $g_m \sim U(\cdot)$ defined on the support $[g_d, g_u]$ and keep this value constant until the next break is generated.

Because the use of weekly data has been common in the empirical option pricing literature (see e.g., Dumas *et al.*, 1998) and also to save computational time without any loss in our qualitative insights, even though in our research design we re-price the stock index and the bond at daily

[19] In addition, using Monte Carlo methods we simultaneously estimate the expected dividend yield and expected zero curves over the residual 'life' of each option contract with the objective of obtaining the necessary inputs for IV computation.

frequency, we calculate option prices across strikes and maturities on the Wednesday of each week, which corresponds to steps of 5 simulated days.[20]

3.3 Qualitative results

The existence of breaks in the fundamentals mean growth rate and the need of investors to learn about such an unstable, time-varying parameter causes non-stationarities in stock, bond, and option prices. These are the core of the ability of a model with incomplete information and rational learning to explain key stylized facts concerning IVs. To get some intuition for the nature of the instabilities captured by our framework, Figure 1 displays one complete simulation path in terms of simulated mean dividend growth rates (g), equilibrium stock prices (S), and at-the-money ($K/S = 1$) short-term (30 calendar days to maturity) implied volatilities (IVATM, Short-T) under our three scenarios (A)-(C) listed above. Equilibrium stock and option prices are computed for the case of α=0.2.[21,22] In the upper panel of the Figure we plot three time series: one is trivially the constant level of g in the absence of breaks; the second, step-like function, corresponds to the time series of g_t when the mean dividend growth rate is affected by infrequent breaks (one can count 7 breaks over the simulation periods, which is realistic in the light of the empirical evidence in Appendix B); the third is the recursive inference on mean dividend growth rate obtained by a rational investor using Bayes' rule based on the empirical likelihood of the data. Looking at this third series, one can notice that learning may occasionally take a long time. Estimates of g_t progressively adjust toward the true values after each break. However, there are also cases in which the investor's estimate of g_t since the most recent break actually drifts away from the fixed but unknown value (see the upper panel around the simulated observation 500). On the one hand, the observable dividend signals received by the investor are noisy because of the presence of an innovation term in the geometric random walk process. Consequently, the agent needs time to learn and thus to

[20] As customary in the empirical literature, the selection of Wednesdays minimizes the incidence of the number of holidays because we simulate according to the actual, authentic CBOE trading calendar between 1996 and 2007.

[21] As simulations replicate option prices in a realistic way that tracks CBOE rules, so that 30-day at-the-money option contracts are not always offered and traded, we calculate IVATM, Short-T IVs by simple linear interpolation using the four contracts around a 30-day time-to-maturity mark and with closest strike price to S.

[22] The lower panel of the figure depicts IVs instead of option prices because the former are easier to interpret and analyse than the underlying option prices, where IVs are extracted from prices using BS. The direct use of option prices is not advisable in comparative analyses due to the fact that option prices differ in their 'level' depending on option contract features.

obtain accurate values for the unknown g_t. On the other hand, in the figure a new break often appears when learning has improved the accuracy of the agent's estimations and hence her cognitive process strengthens once again. Importantly, the simulated real dividends underlying both the complete vs. the incomplete information scenarios in Figure 1 are identical, and the differences are purely due to the need by the investor to learn in the second case.

[Insert Figure 1 here]

The middle panel of Figure 1 shows a particular path for stock prices. Visibly, at least in this particular realized path, the simulated time series of prices in the presence of breaks—both for the complete and incomplete information scenarios—are substantially lower than in the case of no breaks. This result is simply due to the lower g_t values in the scenarios with breaks than in the stationary scenario through the whole simulated period (see Figure 1, upper panel). However, this effect is not structural, in the sense that alternative simulations might have generated different effects, i.e., break-induced stock prices that are higher than no-break equilibrium ones. Finally, the third panel of the figure shows that the occasionally intense revisions of agents' expectations about the (new, post-break) value of g_t induce an increase in IVs, especially in the immediate aftermath of breaks, when the learning speed accelerates and revisions are stronger. The difference recorded between the times series for the case of breaks but complete information and the time series under breaks and learning shows that it is mostly learning and not breaks that are responsible for the elevated IVs and the spikes visible in the third panel. This lower panel also points to the possibility of serial correlation and volatility clustering in option IVs, which is one of the features we focus on in the following. All in all, Figure 1 helps emphasizing that the interaction between learning and breaks may strongly affect both the level and the dynamics of IVs, an indication that option pricing is potentially affected by the induced dynamic premia.

On average, the compounding of the infrequent, limited non-stationarities in fundamentals generated by rational learning effect the deep properties of the security market economy. This is emphasized, for two alternative configurations of the calibration parameters but always with reference to the case of $\alpha = 0.2$ in Table I. In these tables, we report summary statists across simulations for real dividends, for the mean dividend growth rate (observable and constant in one case, and subject to breaks, observable or not in the remaining parts of the tables), the short-term interest rate, the stock price, the short-term at-the-money call price, and its implied

volatility (subject to the same approximations that we have described above). The top panel of Table I concerns the case of low volatility of fundamentals, the lower panel concerns the high volatility case. We report additional summary statistics for fundamentals and asset prices in Appendix D, Table D1, where we also experiment with α set at 0.5 and 5.0 using the same combinations of parameters and scenarios as in Table I.

[Insert Table I here]

Table I show that dividends are exactly the same for all scenarios, as it should be. Breaks just affect the nature of the subordinate process of fundamentals, not its average or median levels. However, breaks inflate the standard deviation and the tail thickness of the dividend distribution. Additionally, it is particularly interesting to observe that the standard deviation of the g_t is higher in the scenario with breaks and complete information than in the case of breaks and learning (for the estimated mean growth), which is easily understood observing the upper panel in Figure 1: under complete information, when mean growth is observable, the plot shows large changes in g_t on breaking dates, where by definition shifts in g_t are immediately recognized by the agent. On the opposite, in the initial periods after a break, in an economy with Bayesian learning, the agent recursively incorporates new information giving some weight to her prior beliefs, and thus producing only gradual movements and smoother adjustments. As already observed, there are no structural differences in the means (of approximately 813-814 index points) and medians (approximately 761-770 index points) of stock prices across alternative scenarios. However, as one would expect—both because dividends are more volatile and because the price-dividend ratio also becomes time-varying—stock prices become more volatile, and slightly more skewed to the right. Correspondingly, as one would expect (see also a proof in GT, 2003, for the case of no breaks), average option prices are higher in the presence of breaks and Bayesian learning. For instance, the average ATM, 1-month call price is 4.4 points in the absence of breaks, 5.4 when observable breaks are introduced, and 12.8 when breaks support a sustained learning process.

A comparison of the first two scenarios in Table I, that describes the cases of complete information with and without breaks, shows that breaks by themselves induce an increase in implied volatilities (for instance, in the top panel from an average of 5% that exactly matches the assumed level of σ to 5.75%). However, this effect is smaller than the impact of the

information incompleteness and learning. For instance, the top (lower) panel shows that IVs increase from 5.75% (31.63%) in the scenario under breaks and full information to 19.24% (43.28%) in the case under breaks and incomplete information with learning. In addition, learning also induces skewness and kurtosis in option prices and implied volatilities that is otherwise absent.

However, the power of learning to induce these realistic features in option prices and IVs is strongly affected by the assumed curvature of the representative investor's utility function. Figure 2 shows the results of a sensitivity analysis using a range of relative risk-aversion levels α applied to *IVS* shape features in an economy under breaks and incomplete information with learning. Figure 2 reports the average behaviour of the IVs of multiple option contracts *one month* after a break in g_t. In Figure 2, the average values of IVs are presented across both the moneyness dimension using short-term option contracts (upper windows) and the maturity dimension by the use of at-the-money option contracts (lower windows). Panels to the right refer to the case of α < 1, while panels to the left to the case α > 1.[23]

[Insert Figure 2 here]

The two upper plots in Figure 2 show that rational learning produces the typical skews of IV/asymmetric "smiles" that have been often reported in the empirical literature: IVs are higher for deep in-the-money calls and—by a simple European put-call parity argument—especially deep out-of-the-money puts. The intuition is that because option prices depend on expectations of future fundamentals in a highly nonlinear way, the effects of Bayesian learning across alternative moneyness levels is asymmetric and—even when option prices have been filtered through BS formula—they create highly asymmetric IV shapes. Additionally, the two upper panels of Figure 2 imply a negative relationship between α and IV levels when $\alpha < 1$, while the relationship turns positive when $\alpha > 1$. The intuition behind these results is simple. Learning has the lowest (zero) impact on stock and option prices when $\alpha = 1$ since the components of the valuation formulas that are affected by any unknown, time-varying parameter g_t disappear (see equations (6) and (14)). In fact, in this case the BS case of a completely flat IVS obtains (unreported in the figure, see GT, 2003). Learning has its strongest

[23] In the case of α = 1, the analysis that has followed Proposition 1 shows that in spite of incomplete information and learning, the price-dividend ratio becomes a constant and learning has no effects (see also Veronesi, 1999, and David, 2008, for similar remarks). Therefore our analysis abstracts from such a limit case.

effects as $\alpha \to 0^{+}$, where it has to be taken into account that existence of the equilibrium requires that the condition $1 + \rho > (1 + g_u)^{1-\alpha}$ has to be always satisfied, which prevents α to be set to zero if $g_u > \rho$, as the absence of arbitrage requires. As α > 1 grows, the effects of learning progressively weaken, but the risk premium associated to market variance grows, and this explains why in the rightmost upper panel, average IV resumes an increasing patter as α > 1 gets larger.

Moreover, the two upper panels of Figure 2 show that when $\alpha < 1$, slopes and curvatures of the IV skews increase with α, which means that IV skews become steeper, while when $\alpha > 1$, slopes and curvatures of implied volatility decrease as α grows, i.e., the IVS flattens in the moneyness dimension. These results are explained by the fact that learning has its strongest effects over in- (out-)of-money call (put) contracts, as already mentioned above. Moreover, as α $\to 1$, the impact of learning on option prices tends to disappear faster for at-the-money and out- (in-)of-money call (put) contracts, at least in relative terms. This causes the IV shapes to display steeper slopes and higher curvatures when $\alpha \to 1$ than in other cases.

The two lower panels of Figure 2 show that learning also induces downward sloping shapes in the IVS as a function of time-to-maturity, as IVs strongly decrease as time-to-maturity increases. Immediately after (Figure 2 takes a picture of BS IVs one month after) a break, there are intense revisions of agents' expectations concerning the new, unknown value of g_t. However, a Bayesian agent expects that she will learn progressively in the future because she will receive further information to make her perception of the mean growth rate of fundamentals increasingly precise. These expectations of future learning reduce the price and hence the IVs of long-term option contracts in relation to short-term option contracts. Furthermore, Figure 2 lower panels emphasize that the IV levels are the lowest when CRRA is close to one. This is explained with reference to the same arguments used above, because learning effects on stock and option prices are nil when $\alpha = 1$. In conclusion, Figure 2 presents evidence to support the claim that our Bayesian learning model is consistent with and explains the large empirical literature that has reported IV variations across moneyness and time-to-maturity (e.g. Rubinstein, 1985; Dumas *et al.*, 1998; Das and Sundaram, 1999).

Figure 3 reports a sensitivity analysis concerning the effects of the CRRA parameter α similar to Figure 2. However, differently from Figure 2, Figure 3 concerns the average behaviour of IVs

as a function of moneyness and time-to-maturity *one year* after a break in g_t. The choice of one year corresponds to the fact that, as we have seen in Section 3.1, our empirical estimates indicate that the average duration of a given regime as defined by the current value of g_t should be of approximately one year. The comparative analysis of Figures 2 and 3 allows us to make comments on the varying learning effects on the IVS over time. They show that the average level of IVs decreases as more information is received since the last observed break. This is caused by the fact that the speed of learning and, consequently, its effects weaken when an investor has received a growing amount of dividend signals that ought to allow her to form relatively precise inferences concerning g_t. Nevertheless, and differently from earlier papers, such as GT (2003), the effects of learning never disappear altogether, even after one year since the most recent break. Moreover, the upper rightmost panel of Figure 3 shows when plotted as a function of moneyness, IVs describe convex functions for α values close to one when $\alpha > 1$; however, as α increases, the IV shapes describe concave curves. The main reason for these concave shapes is that when $\alpha > 1$, representative agent, endowment-based asset pricing models in general display a counter-intuitive feature by which stock prices are lower when g_t increases (see Abel, 1988; Cecchetti *et al.*, 1990). This odd effect, that in any event takes place only when learning is weak, induces these concave IV shapes in the moneyness dimension.[24]

[Insert Figure 3 here]

3.4 Quantitative analysis

Besides using the qualitative methods and intuition in Figures 2-3 and Table I, we also employ statistical methods to quantify the effects of breaks and learning under incomplete information on both the dynamics of the IVS. Table II computes such dynamic features for IVs as well as the IVS shape movements from simulations concerning an economy characterized by infrequent breaks and incomplete information. Such features are represented by means of simulation-specific moments (e.g., means, standard deviations, serial correlations, and ARCH coefficients). In the case of serial correlation and ARCH(q) tests, besides the average of the corresponding test statistics across simulations, the percentages in parentheses appearing in Table II are

[24] Despite this counter-intuitive feature of dynamic equilibrium models when $\alpha > 1$, we include them in our analyses to be consistent with the large literature in which $\alpha > 1$ has been estimated or used to explain properties of asset prices not of a direct concern to our paper.

computed as the fraction of the total number of simulation trials that imply Ljung-Box and ARCH Lagrange multiplier tests with p-values of 0.1 or lower. The results presented in Table II are obtained from simulations using two different parameter setups, the same that have appeared already in Table I. However in appendix D, Tables D2 – D3 show simulation results for additional parameter combinations as a robustness check. We define $Slope_{Mon}$ ($Slope_{Mat}$) as the average across simulation trials of numerical first derivatives with respect to moneyness (time to maturity) computed from all the pairs of priced options with neighbouring moneyness levels and 30 days to maturity (neighbouring maturity levels and closest at-the-money). In addition, $Curv_{Mon}$ ($Curve_{Mat}$) is the average across simulation trials of numerical second derivatives with respect to moneyness (time to maturity) computed from all triplets of priced options with neighbouring moneyness levels and 30 days to maturity (neighbouring maturity levels and closest at-the-money).[25,26]

Table II shows that, on average, learning induces negative slopes and convex IV shapes in both the moneyness and maturity dimensions. Moreover, rational learning generates kurtosis, serial correlation, and volatility clustering in both the IVs themselves and in the slope and curvature indices computed from the simulated IVS. The levels of IV as well as all the shape features that describe the IVS imply a large and significant serial correlation coefficient in more than 50% of the simulations using a first-order Box-Pierce test statistic. This means that higher IV today, a steeper negative IVS slope, or a more convex IVS shape all forecast high IV levels, negative slopes and convex IVS shapes in the future. Furthermore, the IV level, the slopes and curvatures of the IVS under learning imply on average widespread volatility clustering as measured by the percentage of significant ARCH LM tests (both with one and with three lags). This means that when IV levels, slope or convexity of the IVS become variable over time, this instability tends to persist over time. However, ARCH effects are weaker in the case of the slope

[25] A numerical first derivative is simply defined as $f'(x_1) \equiv (f(x_1) - f(x_0))/(x_1 - x_0)$; a numerical second derivative is instead $f''(x_1) \equiv (f(x_2) - 2f(x_1) + f(x_0))/(0.5(x_2 - x_0))^2$.

[26] An alternative way to characterize the IVS shape and its dynamics is through deterministic IVS models, which describe the implied volatilities as a function of an option strike price and time-to-maturity (see Dumas *et al.*, 1998). Moreover, these polynomial functional forms have been successfully used to capture the presence of predictability in the shape of the IVS itself (e.g., Gonçalves and Guidolin, 2006). However, deterministic IVS models impose cross-sectional relationships among different factors that could add noise to the analysis of our theoretical equilibrium model. Instead, we prefer the simplicity of numerical derivatives which are calculated independently in each of the two IVS dimension (i.e., moneyness and maturity). However, as a robustness check, in Appendix E we also assess whether a rational learning model may produce deterministic IVS estimates comparable to those commonly found in the literature.

and curvature indices measured with respect to moneyness, $Slope_{Mon}$ and $Curve_{Mon}$, although 10% statistical significance is preserved for at least 20% of the simulations.

[Insert Table II here]

The results presented in Table II are consistent with the empirical evidence reported in the literature about the predictable dynamics in the *IVS* (e.g., Harvey and Whaley, 1992; Gonçalves and Guidolin, 2006; Fengler *et al.*, 2007; Konstantinidi *et al.*, 2008). To provide evidence that a model with breaks and Bayesian learning on the unobservable growth rate of fundamentals, Table III has the same structure as Table II but it is no longer based on simulated option prices. On the contrary, Table III concerns a large set of actually traded, non-zero volume stock options sampled between 1997 and 2007. In particular, panel A of Table III concerns IV levels and IVS shape and predictability patterns measured on S&P 500 index options; panel B, covers instead similar statistics with reference to a set of 150 individual equity options in which the underlying stocks pays dividends.[27] The options data used to compute the statistics reported in Table III are described in Appendix C. The predictability patterns in the IVS which are shown in Tables II and III show the strong similarities between the empirical properties of the data and the features that emerge from the rational learning model with infrequent breaks introduced in Section 2 and simulated in this Section. For instance, S&P 500 data deliver an average ATM, 1-month to maturity IV of 16.7% vs. 19.2% from our simulations, under the first set of (low volatility, σ = 5%) parameters; the empirical slope (curvature) index in the moneyness dimension is -0.64 (13.8) in the data and -0.35 (30.9) in our simulations. Therefore the signs are always correct, although a model with learning yields IVS shapes vs. moneyness that are considerably more convex than what can be detected in S&P 500 data. Results are less accurate in the case of IVS shapes vs. time to maturity, because the empirical slope (curvature) index in the time to maturity dimension is 0.03 (-0.12) in the data and -0.31 (3.28) in our simulations,

[27] Although equity options are American-style, there is empirical evidence that they follow similar IVS dynamics as European contracts such as S&P 500 index options (see, e.g., Dennis and Mayhew, 2002; Goyal and Saretto, 2009; Bernales and Guidolin, 2012). In addition, possible small biases and heterogeneities across panels A and B probably carry modest importance when compared to the enormous benefits we may obtain from observing the rich cross-sectional dynamic behaviours by the use of 150 different equity options.

and the last sign appears to be incorrect, while it is realistic that IVS be approximately flat when plotted against maturity.[28]

Such an ability for a simple dynamic equilibrium model with breaks and Bayesian learning to re-produce the shape of the IVS extends also to a cross-section of individual equity options as shown by a comparison between the second (low volatility, σ = 30%) calibration in Table II, panel B and panel B in Table III. In this case, at least qualitatively, all the key properties of the (average) IVS from U.S. options markets are matched by our simulations. The data show an average ATM, 1-month to maturity IV of 40.3% vs. 43.3% from our simulations; the empirical, numerically computed slope (curvature) index in the moneyness dimension is -0.21 (2.62) in the data and -0.19 (2.87) in our simulations; the empirical slope (curvature) index in the time to maturity dimension is -0.04 (0.08) in the data and -0.31 (3.53) in our simulations.

[Insert Table III here]

The rightmost sections of Tables II and III are instead devoted to the predictability and instability of the IVS shape and level. Empirically, for both S&P 500 and individual equity options data, the average IV level tends to be highly (and positively) persistent; for instance, for 98% of the short-term ATM individual option series, the null of no serial correlation can be rejected. This is fully mimicked by our calibrated results, where for both sets of parameters in Table II, 98.8 and 93.3% of the simulations reveal statistically significant autocorrelations in IV levels, an indication that a high positioning of the IVS today forecasts the same for the following weeks. A similar finding holds with reference to both slope and convexity indicators in the case of S&P 500 options, which is fully captured by the properties of simulated IV series from our model. Interestingly, in the case of individual equity options, there is strong evidence of serial correlation in slope and curvature of the IVS in the time-to-maturity dimension, while there little evidence in the data of similar phenomena vs. moneyness. The second set of calibration parameters can then reproduce such a persistence in slope and curvature indices in the maturity dimension, although it also tends to create excessive persistence in the moneyness one. Similar results appear as far any volatility clustering—i.e., the persistence of instability in the very shape of the IVS that when rapidly changing would tend to remain so for a few

[28] However, below we show that also empirically, when there are high levels of uncertainty (when learning speed is high in the aftermath of a structural break) in S&P 500 index options, maturity slopes tend to be negatively sloped which is consistent with our calibration results.

consecutive weeks—is concerned: the calibration in panel A of Table II well matches most of the results concerning S&P 500 IVS dynamics; interestingly, the calibration in panel B of Table II is also able to capture the evidence in individual equity options that ARCH effects would weak as far slope and convexity indices are concerned in the maturity dimension.

An agent's learning process also affects how the level of implied volatility and the IVS shape characteristics are related to each other in a cross-sectional sense, for instance whether slope and convexity in the moneyness dimension tends to lower (i.e., the IVS is flatter) when the entire level of the IVS shifts upwards, which is empirically the case. For instance, Mixon (2007) has found that the slope of at-the-money IV over different maturities has predictive ability for the level of future short-dated IV (although not to the extent predicted by a simple expectations hypothesis). To examine this interesting and delicate effects, Tables *IV* (we use the italics to prevent any confusion with the acronym "IV") and V show the matrices of cross-indicator simultaneous correlations in our calibrations (Table *IV*) and in the data (Table V). Also in this case, two different sets of parameters appear in Table *IV* while in Table V we report estimated correlation coefficients for S&P 500 and the average across 150 distinct individual stock options, respectively. Nevertheless in Appendix D, Tables D2-D3, we report further correlation analyses using alternative parameterizations, as a robustness check.

Once more, the fit provided by our model with infrequent breaks and incomplete information to the empirical properties of the IVS estimated from the U.S. options market is impressive. Table V reveals a number of non-zero and statistically significant cross-correlations. For instance, in panel B, the IVS becomes flatter (the slope less negative and the smile weaker) in the moneyness dimension as well as more negatively sloped by more convex in the maturity dimension, when the general level of the IVS shifts up. Or, the IVS becomes steeper vs. moneyness when at the same time it becomes steeper (flatter) in the maturity dimension. A steeper negative slope as a function of maturity tends to be accompanied by less convexity (i.e., the term structure of the IVS tends to approximate a negative sloped line, that however approaches smoothly and asymptotically the zero axis for very high maturities). An inspection of the estimated correlations among these properties of the IVS in Table *IV* reveals that most of these features are well captured by our model, especially in the high-volatility calibration reported in panel B.

[Insert Table IV here]

[Insert Table V here]

We conclude that although far from perfect, even a simple and yet powerful general equilibrium asset pricing model such as ours is capable of capturing not only the key properties of option prices and IVs (as shown to some extent already in GT, 2003, and David and Veronesi, 2009), but also the dynamics revealed in the entire IVS, both as a function of moneyness and vs. the maturity dimension.

4 Conclusions

The fact that option prices and especially (BS) implied volatilities are predictable has been identified by academics and exploited by practitioners in a number of valuable applications, from hedging to trading. Nevertheless, there is a gap in the literature regarding possible explanations for such puzzling predictability patterns. In fact, under the simplest option pricing benchmark, the ineffable Black-Scholes pricing models and its simple extensions, the IVS would be flat and not moving over time. Also more complex pricing frameworks that go well beyond the simplistic assumptions underlying BS, are usually silent about the specific features of the dynamics in the IVS. In this paper, we contribute to this body of literature by finding evidence to support the hypothesis that the investors' learning plays an important role in explaining the commonly reported dynamic predictability patterns characterizing the IVS.

We present an equilibrium model in which the fundamental mean dividend growth rate (the drift of the corresponding stochastic process) is subject to infrequent but observable breaks, that therefore occur only with a small probability. Under incomplete information—which represents the realistic description of the world in which deep parameters and mean growth rates may at best be estimated—a representative agent receives independent but noisy daily signals about the unknown fundamental value that are efficiently used to update her beliefs about the unobservable mean growth rate using a Bayesian updating algorithm.

We show that learning explains several anomalies in the form of predictability patterns for option prices and the IVS that have been commonly reported in the empirical literature. Rational learning makes agents' beliefs time-varying and in equilibrium this leads to the

existence of sizable dynamic risk premia that affect both option prices as well as the movements of the (BS) volatilities implicit in such prices (see e.g., Mixon, 2007). Moreover, our modelling approach shows that learning generates heterogeneous dynamic properties for option contracts depending of their moneyness and residual maturity; these heterogeneous effects, due to the complex shape of the perceived, time-varying pricing kernel under rational learning is responsible for the (non-flat) and predictable shape of the IVS. In particular, a quantitative calibration of the model under a variety of alternative settings (a few of them collected in Appendix D to provide further robustness checks) shows that the very shapes, slopes, and curvatures—both vs. moneyness and maturity—properties of empirically estimated IV surfaces can be easily reproduced in almost their entirety by the Bayesian learning pricing model.

One aspect of our model may also teach a more general lesson to scholars in the field. Option markets have been widely used to capture forward-looking information since they reflect agents' expectations about future scenarios, in which forecasting horizons match the expiration dates of options contracts (see Fleming, 1998). The information captured from option prices has been used by investors in a range of markets and with applications to a broad spectrum of financial issues including risk management, asset allocation, and capital budgeting.[29] However, through our model we also show that option markets may display not only the classical, forward-looking features; it is also realistic to think that they are at the same time affected by backward-looking characteristics since also option traders need to learn recursively as new information arrives. Participants in option markets face a sequential process of information acquisition in which signals are received and processed with reference to the historical information and prior beliefs. Therefore, the forward-looking information obtained from option markets is generated by a backward-looking learning process. Such tight intertwining between backward- and forward-looking information processing imposes useful restrictions that ought to be carefully considered and tested when models of option pricing are quantitatively assessed.

[29] For instance, option prices have been used to forecast underlying returns (e.g.,see, Xing *et al.*, 2010; Cremers and Weinbaum, 2010; and Bakshi *et al.*, 2011), realized volatilities (e.g., Christensen and Prabhala,1998; Busch *et al.*, 2011), betas (e.g., Siegel, 1995; Chang *et al.*, 2009), correlations (e.g., Driessen *et al.*, 2009), and to estimate the moments required in standard asset allocation problems (e.g., Kostakis *et al.*, 2011; DeMiguel *et al.*, 2012).

Finally, our model is simple and intuitive. Just because of this reason it may extended in a variety of directions at the same time preserving its key intuition that any dynamics in the IVS may be consistent with no arbitrage pricing restrictions and instead derive from time-varying risk premia that compensate investors for the additional risk deriving from belief revisions at a varying speed due to the infrequent occurrence of breaks. For instance, the model could be used to isolate the portion of variation in the IVS that is due to rational pricing factors from those that are simply irrational (see e.g., Kim and Lee, 2013). Moreover, a literature exists that has investigated the properties of option returns (see, e.g., Broadie *et al.*, 2009) and detected a number of difficult to solve anomalies with reference to standard asset pricing frameworks. It seems interesting to further investigate how rational learning would affect such pricing framework and whether this may teach us something about the nature of option returns.

References

Abel, A., 1988, Stock prices under time-varying dividend risk: An exact solution in an infinite-horizon general equilibrium model, *Journal of Monetary Economics* 22, 375-393.

Bai, J., R. Lumsdaine, and J. Stock, 1998, Testing for and Dating Common Breaks in Multivariate Time Series, *Review of Economic Studies* 63, 395-432.

Bakshi, G., G. Panayotov, and G. Skoulakis, 2011, Improving the predictability of real economic activity and asset returns with forward variances inferred from option portfolios, *Journal of Financial Economics* 100, 475-495.

Beber, A., and M. W. Brandt, 2006, The effect of macroeconomic news on beliefs and preferences: Evidence from the options market, *Journal of Monetary Economics* 53, 1997-2039.

Beber, A., and M. W. Brandt, 2009, Resolving macroeconomic uncertainty in stock and bond markets, *Review of Finance* 13, 1-45.

Bernales, A., and M. Guidolin, 2012, Can we forecast the implied volatility surface dynamics of equity options?, Working paper, Banque de France.

Black, F., and M., Scholes, 1973, The pricing of options and corporate liabilities, *Journal of Political Economy* 81, 637-654.

Bray, M., and D. Kreps, 1987, Rational learning and rational expectations. In: Feiwel, G. (Ed.), Arrow andthe Ascent of Modern Economic Theory. New York University Press, New York.

Brennan, M., and H. Cao, 1996, Information, trade, and derivative securities, *Review of Financial Studies* 9, 163-208.

Broadie, M., M., Chernov, and M. Johannes, 2009, Understanding Index Option Returns, *Review of Financial Studies* 22 4493-4529.

Busch ,T., B. J. Christensen, and M. Ø. Nielsen, 2011, The role of implied volatility in forecasting future realized volatility and jumps in foreign exchange, stock, and bond markets, *Journal of Econometrics* 160, 48-57.

Cecchetti, S. G., P. Lam, and N. C. Mark, 1990, Mean reversion in equilibrium asset prices, *American Economic Review* 80, 221-242.

Chalamandaris, G., and A.E. Tsekrekos, 2010, Predictable dynamics in implied volatility surfaces from OTC currency options, *Journal of Banking and Finance* 34, 1175-1188.

Chang, B. Y., P. Christoffersen, K. Jacobs, and G. Vainberg, 2009, Option-implied measures of equity risk, Working paper, McGill University.

Christensen, B. J., and N. Prabhala, 1998, The Relation Between Implied and Realized Volatility, *Journal of Financial Economics* 50, 125-150.

Christoffersen, P.F., S. Heston, and K. Jacobs, 2009, The shape and term structure of the index option smirk: Why multifactor stochastic volatility models work so well, *Management Science* 55, 1914-1932.

Chu, C. S. J. , M. Stinchcombe, and H. White, 1996, Monitoring structural change, *Econometrica* 64, 1045-1065.

Cremers, M., and D. Weinbaum, 2010, Deviations from put-call parity and stock return predictability, *Journal of Financial and Quantitative Analysis* 45, 335-367.

Das, S., and R. Sundaram, 1999, Of smiles and smirks: A term structure perspective, *Journal of Financial and Quantitative Analysis* 34, 211-239.

David, A., 2008, Heterogeneous Beliefs, Speculation, and the Equity Premium, *Journal of Finance* 63, 41–83.

David, A., and P. Veronesi, 2009, Option prices with uncertain fundamentals, Working paper, University of Chicago.

DeMiguel, V., Y., Plyakha, R., Uppal, and G. Vilkov, 2012, Improving portfolio selection using option-implied volatility and skewness, *Journal of Financial and Quantitative Analysis*, forthcoming.

Dennis, P., and S. Mayhew, 2002, Risk-neutral skewness: Evidence from stock options, *Journal of Financial and Quantitative Analysis* 37, 471-493.

Donders, M., R. Kouwenberg, and T. Vorst, 2000, Options and earnings announcements: An empirical study of volatility, trading volume, open interest, and liquidity, *European Financial Management* 6, 149–172.

Driessen, J., P. J. Maenhout, and G. Vilkov, 2009, The price of correlation risk: Evidence from equity options, *Journal of Finance* 64, 1377-1406.

Duan, J. C., and J. G. Simonato, 2001, American option pricing under GARCH by a Markov chain approximation, *Journal of Economic Dynamics and Control* 25, 1689-1718.

Dubinsky, A., and M. Johannes, 2006, Earnings announcements and equity options, Working paper, Columbia University.

Dumas, B., J. Fleming, and R. Whaley, 1998, Implied volatility functions: Empirical tests, *Journal of Finance* 53, 2059-2106.

Ederington, L., and J. H. Lee, 1996, The creation and resolution of market uncertainty: The impact of information releases on implied volatility, *Journal of Financial and Quantitative Analysis* 31, 513-539.

Fengler, M., 2009, Arbitrage-free smoothing of the implied volatility surface, *Quantitative Finance* 9, 417-428.

Fengler, M.R., W.K. Härdle, and E. Mammen, 2007, A semiparametric factor model for implied volatility surface dynamics, *Journal of Financial Econometrics* 5, 189-218.

Fleming J., 1998, The quality of market volatility forecasts implied by S&P 100 index option prices, *Journal of Empirical Finance* 5, 317-345.

Gonçalves, S., and M. Guidolin, 2006, Predictable dynamics in the S&P 500 index options implied volatility surface, *Journal of Business* 79, 1591-1635.

Goyal, A., and A. Saretto, 2009, Cross-section of option returns and volatility, *Journal of Financial Economics* 94, 310-326.

Granger, C. and N. Hyung, 2004, Occasional structural breaks and long memory with an application to the S&P 500 absolute stock returns, *Journal of Empirical Finance* 3, 399-421.

Guidolin, M., 2006, High equity premia and crash fears. Rational foundations. *Economic Theory* 28, 693–708.

Guidolin, M., and A. Timmermann, 2003, Option prices under Bayesian learning: Implied volatility dynamics and predictive densities, *Journal of Economic Dynamics and Control* 27, 717-769.

Guidolin, M., and A. Timmermann, 2007, Properties of equilibrium asset prices under alternative learning schemes, *Journal of Economic Dynamics and Control* 31, 161-217.

Harvey, C. R., and R. E. Whaley, 1992, Market volatility prediction and the efficiency of the S&P 100 index option market, *Journal of Financial Economics* 31, 43-73.

Heston, S., and S. Nandi, 2000, A closed-form GARCH option valuation model, *Review of Financial Studies* 13, 585-625.

Huang, C. F., and R. H. Litzenberger, 1988, *Foundations for Financial Economics* (North-Holland, The Netherlands).

Kim N., and J. Lee, 2013, No-arbitrage implied volatility functions: Empirical evidence from KOSPI 200 index options, *Journal of Empirical Finance* 21, 36-53.

Kleidon, A. W., 1986, Variance bounds tests and stock price valuation models, *Journal of Political Economy* 94, 953-1001.

Konstantinidi, E., G. Skiadopoulos, and E. Tzagkaraki, 2008, Can the evolution of implied volatility be forecasted? Evidence from European and US implied volatility indices, *Journal of Banking and Finance* 32, 2401-2411.

Kostakis, A., N. Panigirtzoglou, G. Skiadopoulos, 2011. Market timing with option-implied distributions: A forward-looking approach, *Management Science*, forthcoming.

Leisch, F., K. Hornik, and C. M. Kuan, 2000, Monitoring structural changes with the generalized fluctuation test, *Econometric Theory* 16, 835-854.

Lettau, M., and S. Van Nieuwerburgh, 2008, Reconciling the return predictability evidence, *Review of Financial Studies* 21, 1607-1652.

Lucas, R., 1978, Asset prices in an exchange economy, *Econometrica* 46, 1429-1445.

Mixon, S., 2007, The implied volatility term structure of stock index options, , *Journal of Empirical Finance* 14, 333–354.

Ni, S. X., J. Pan, and A. M. Poteshman, 2008, Volatility information trading in the option market, *Journal of Finance* 63, 1059–1091.

Pastor, L., and R. F. Stambaugh, 2001, The equity premium and structural breaks, *Journal of Finance* 56, 1207-1239.

Pliska, S. R., 1997, *Introduction to Mathematical Finance* (Blackwell, Oxford).

Rubinstein, M., 1976, The Valuation of Uncertain Income Streams and the Pricing of Options, *Bell Journal of Economics* 7, 407-425.

Rubinstein, M., 1985, Nonparametric tests of alternative option pricing models using all reported trades and quotes on the 30 most active CBOE option classes from August 23, 1976 through August 31, 1978, *Journal of Finance* 40, 455-480.

Rubinstein, M., 1994, Implied binomial trees, *Journal of Finance* 49, 771–818.

Shaliastovich, I., 2008, Learning, confidence and option prices, Working paper, Duke University.

Siegel, A. F., 1995, Measuring systematic risk using implicit beta, *Management Science* 41,124-128.

Timmermann, A., 1993, How learning in financial markets generates excess volatility and predictability of excess returns, *Quarterly Journal of Economics* 108, 1135-1145.

Timmermann, A., 1996, Excess volatility and predictability of stock prices in autoregressive dividend models with learning, *Review of Economic Studies*, 63, 523-557.

Timmermann, A., 2001, Structural breaks, incomplete information, and stock prices. *Journal of Business and Economic Statistics* 19, 299-314.

Xing, Y., X. Zhang, and R. Zhao, 2010, What does individual option volatility smirk tell us about future equity returns?, *Journal of Financial and Quantitative Analysis* 45, 641-662.

Yan, S., 2011, Jump risk, stock returns, and slope of implied volatility smile, *Journal of Financial Economics* 99, 216-233.

Appendix A: Proofs

Proof of Proposition 1: Assuming that the expression that describes S_t^{CI} can be written as $S_t^{CI} = D_t\Psi(g_t)$ for some function $\Psi_t^{CI}(\cdot)$, we define a "break indicator", s_t, that signals the occurrence of breakpoints in the mean dividend growth rate. In the case in which there is no break in g_{t+1} $s_{t+1} = s_t$; if instead $s_{t+1} = s_t + 1$, then a break has taken place at $t+1$. Additionally, $\Pr(s_{t+1} = s_t) = (1-\pi)$ is the probability of no break, and the probability of a break out of the state prevailing at time t is $\Pr(s_{t+1} = s_t + 1) = \pi$. Therefore, from equation (4):

$$
\begin{aligned}
&(1+\rho)\Psi(g_t)D_t \\
&\qquad = \sum\nolimits_{\mathrm{i}=0}^{1} E_t\left[(\Psi_t^{CI}(g_t)D_{t+1} + D_{t+1})\left(\frac{D_{t+1}}{D_t}\right)^{-\alpha} | s_{t+1} = s_t + \mathrm{i}\right]\Pr(s_{t+1} = s_t + i) \\
&= (1-\pi)\, D_t \int_{-\infty}^{\infty}\left(1 + \Psi_t^{CI}(g_t)\right)(1+g_t)^{1-\alpha}\exp\left((1-\alpha)\left(\sigma\varepsilon_{t+1} - \frac{\sigma^2}{2}\right)\right) \\
&\cdot \phi(\varepsilon_{t+1}|\sigma^2)d\varepsilon_{t+1} + (1-e^{-\pi})D_t \int_{g_d}^{g_u}\int_{-\infty}^{\infty}(1+\Psi_t^{CI}(g_{t+1}))\,(1+g_{t+1})^{1-\alpha} \qquad \text{(A1)} \\
&\cdot \exp\left((1-\alpha)\left(\sigma\varepsilon_{t+1} - \frac{\sigma^2}{2}\right)\right)\phi(\varepsilon_{t+1}|\sigma^2)\, d\varepsilon_{t+1}dG(g_{t+1})
\end{aligned}
$$

where $G(\cdot)$ is the c.d.f. of g_{t+1} defined on $[g_d, g_u]$, ε_{t+1} is the innovation term of the geometric random walk process for dividends, and $\phi(\cdot\,|\sigma)$ is a normal density function with mean zero and variance σ. Therefore, given that ε_{t+1} and g_{t+1} are independent, we can rewrite equation (A1) as:

$$
\begin{aligned}
&(1+\rho)\Psi(g_t)D_t = (1-\pi)D_t(1+g_t)^{1-\alpha}\left(1 + \Psi_t^{CI}(g_t)\right) \\
&+ \pi D_t \int_{g_d}^{g_u}(1+g_{t+1})^{1-\alpha}dG(g_{t+1}) \; + \pi D_t \int_{g_d}^{g_u}\Psi_t^{CI}(g_{t+1})(1+g_{t+1})^{1-\alpha}dG(g_{t+1}) \qquad \text{(A2)}
\end{aligned}
$$

-or equivalently,

$$
\begin{aligned}
D_t\Psi(g_t) &= (1-\pi)\frac{D_t}{1+\rho-(1-\pi)(1+g_t)^{1-\alpha}}(1+g_t)^{1-\alpha} \\
&+ \pi\frac{D_t}{1+\rho-(1-\pi)(1+g_t)^{1-\alpha}}\int_{g_d}^{g_u}(1+g_{t+1})^{1-\alpha}dG(g_{t+1}) \\
&+ \pi\frac{D_t}{1+\rho-(1-\pi)(1+g_t)^{1-\alpha}}\int_{g_d}^{g_u}\Psi_t^{CI}(g_t)(1+g_{t+1})^{1-\alpha}dG(g_{t+1}).
\end{aligned} \tag{A3}
$$

Because $G(\cdot)$ does not vary over time in equation (A3), we multiply both sides by $(1+g_{t+1})^{1-\alpha}dG(g_{t+1})/D_t$ and integrate over $[g_d, g_u]$, to obtain:

$$
\begin{aligned}
&\int_{g_d}^{g_u}\Psi(g_t)(1+g_t)^{1-\alpha}dG(g_t) = \int_{g_d}^{g_u}(1-\pi)\frac{(1+g_t)^{2-2\alpha}}{1+\rho-(1-\pi)(1+g_t)^{1-\alpha}}dG(g_t) \\
&+ \int_{g_d}^{g_u}\pi\frac{(1+g_{t+1})^{1-\alpha}\int_{g_d}^{g_u}(1+g_{t+1})^{1-\alpha}dG(g_{t+1})}{1+\rho-(1-\pi)(1+g_{t+1})^{1-\alpha}}dG(g_{t+1}) \\
&+ \int_{g_d}^{g_u}\pi\frac{(1+g_{t+1})^{1-\alpha}}{1+\rho-(1-\pi)(1+g_{t+1})^{1-\alpha}}dG(g_{t+1}) \\
&\cdot \int_{g_d}^{g_u}\Psi(g_{t+1})(1+g_{t+1})^{1-\alpha}dG(g_{t+1}).
\end{aligned} \tag{A4}
$$

The term on the left side is equal to the second part of last term on the right side, and consequently:

$$
\begin{aligned}
&\int_{g_d}^{g_u}\Psi(g_{t+1})(1+g_{t+1})^{1-\alpha}dG(g_{t+1}) \\
&\qquad = \left(\int_{g_d}^{g_u}(1-\pi)\frac{(1+g_{t+1})^{2-2\alpha}}{1+\rho-(1-\pi)(1+g_{t+1})^{1-\alpha}}dG(g_{t+1})\right. \\
&\left. + \int_{g_d}^{g_u}\pi\frac{(1+g_{t+1})^{1-\alpha}\int_{g_d}^{g_u}(1+g_{t+1})^{1-\alpha}dG(g_{t+1})}{1+\rho-(1-\pi)(1+g_{t+1})^{1-\alpha}}dG(g_{t+1})\right) \\
&/\left(1-\int_{g_d}^{g_u}\pi\frac{(1+g_{t+1})^{1-\alpha}}{1+\rho-(1-\pi)(1+g_{t+1})^{1-\alpha}}dG(g_{t+1})\right).
\end{aligned} \tag{A5}
$$

Finally, inserting equation (A5) into equation (A3), we have:

$$S_t^{CI} = \frac{D_t}{1+\rho-(1-\pi)(1+g_t)^{1-\alpha}} \Bigg\{ (1-\pi)(1+g_t)^{1-\alpha} + \pi \int_{g_d}^{g_u} (1+g_{t+1})^{1-\alpha} dG(g_{t+1}) + \pi \Bigg(\int_{g_d}^{g_u} (1-\pi) \frac{(1+g_{t+1})^{2-2\alpha}}{1+\rho-(1-\pi)(1+g_{t+1})^{1-\alpha}} dG(g_{t+1}) + \int_{g_d}^{g_u} \pi \frac{(1+g_{t+1})^{1-\alpha} \int_{g_d}^{g_u} (1+g_{t+1})^{1-\alpha} dG(g_{t+1})}{1+\rho-(1-\pi)(1+g_{t+1})^{1-\alpha}} dG(g_{t+1}) \Bigg) \Bigg/ \Bigg(1 - \int_{g_d}^{g_u} \pi \frac{(1+g_{t+1})^{1-\alpha}}{1+\rho-(1-\pi)(1+g_{t+1})^{1-\alpha}} dG(g_{t+1}) \Bigg) \Bigg\}. \tag{A6}$$

The integrals in equation (A6) are constant over time and can be labelled as:

$$I_1 = \int_{g_d}^{g_u} (1+g_{t+1})^{1-\alpha} dG(g_{t+1}) \tag{A7}$$

3

$$I_2 = \int_{g_d}^{g_u} \frac{(1+g_{t+1})^{2-2\alpha}}{1+\rho-(1-\pi)(1+g_{t+1})^{1-\alpha}} dG(g_{t+1}) \tag{A8}$$

$$I_3 = \int_{g_d}^{g_u} \frac{(1+g_{t+1})^{1-\alpha}}{1+\rho-(1-\pi)(1+g_{t+1})^{1-\alpha}} dG(g_{t+1}) \tag{A9}$$

and as a result one can see that

$$\begin{aligned} S_t^{CI} &= \frac{D_t}{1+\rho-(1-\pi)(1+g_t)^{1-\alpha}} \Bigg\{ (1-\pi)(1+g_t)^{1-\alpha} + \pi I_1 + \pi \left(\frac{(1-\pi) I_2 + \pi I_1 I_3}{1-\pi I_3} \right) \Bigg\} \\ &= \frac{D_t}{1+\rho-(1-\pi)(1+g_t)^{1-\alpha}} \left\{ (1-\pi)(1+g_t)^{1-\alpha} + \pi \left(\frac{I_1 + (1-\pi) I_2}{1-\pi I_3} \right) \right\}. \end{aligned} \tag{A10}$$

Therefore, equation (A10) shows that $S_t^{CI} = D_t \Psi_t^{CI}(g_t)$, as we state in equation (A1).

In the case of the bond, we use the second Euler equation (5) to obtain:

$$B_t^{CI} = \frac{1}{(1+\rho)} \sum_{i=0}^{1} \mathrm{E}_t \left[\left(\frac{D_{t+1}}{D_t} \right)^{-\alpha} | s_{t+1} = s_t + \mathrm{i} \right] \Pr(s_{t+1} = s_t + i)$$

$$= \frac{1}{(1+\rho)} \left\{ (1-\pi) \int_{-\infty}^{\infty} (1+g_t)^{-\alpha} \exp\left(-\alpha \left(\sigma \varepsilon_{t+1} - \frac{\sigma^2}{2} \right) \right) \phi(\varepsilon_{t+1} | \sigma^2) d\varepsilon_{t+1} + \pi \right.$$

$$\cdot \int_{g_d}^{g_u} \int_{-\infty}^{\infty} (1+g_{t+1})^{-\alpha} \exp\left(-\alpha\left(\sigma\varepsilon_{t+1} - \frac{\sigma^2}{2}\right)\right) \phi(\varepsilon_{t+1}|\sigma^2)\, d\varepsilon_{t+1} dG(g_{t+1}) \Bigg\}$$
$$= \frac{1}{(1+\rho)} \left\{ (1-\pi)(1+g_t)^{-\alpha} + \pi \int_{g_d}^{g_u} (1+g_{t+1})^{-\alpha} dG(g_{t+1}) \right\}. \quad \text{(A11)}$$

The last equality derives from the fact that $G(\cdot)$ does not vary over time and by the independence of ε_{t+1} and g_{t+1}. □

Proof of Proposition 2: The result can be obtained from no-arbitrage arguments applied to a European contingent claim with terminal value given by $\max\{S_{t+\tau}^{CI} - K\}$, when the mean dividend growth rate underlying the pricing of $S_{t+\tau}^{CI}$ is subject to breaks. Therefore, it is necessary to proceed to the risk-neutralization of the probabilities that enter the state price density. Following Huang and Litzenberger (1988, p. 229), we take the Euler equation (4) and divide it by the price of a one-period zero-coupon bond:

$$\frac{(1+\rho) S_{t+k}^{CI}}{(1-\pi)(1+g_{t+k})^{-\alpha} + \pi \int_{g_d}^{g_u} (1+g_{t+k})^{-\alpha} dG(g_{t+k})} = \mathrm{E}_{t+k}\left[\beta \left(\frac{D_{t+k+1}}{D_{t+k}}\right)^{-\alpha} \right.$$
$$\left. \cdot (S_{t+k+1}^{CI} + D_{t+k+1}) \frac{(1+\rho)}{(1-\pi)(1+g_{t+k})^{-\alpha} + \pi \int_{g_d}^{g_u} (1+g_{t+k})^{-\alpha} dG(g_{t+k})} \right]. \quad \text{(A12)}$$

It turns out that the forward price and the forward cumulative dividend process are:

$$S_{t+k}^{CI^*} = \frac{(1+\rho) S_{t+k}^{CI}}{(1-\pi)(1+g_{t+k})^{-\alpha} + \pi \int_{g_d}^{g_u} (1+g_{t+k})^{-\alpha} dG(g_{t+k})} \quad \text{(A13)}$$

and

$$D_{t+k}^{*} = \sum_{s=0}^{k} D_{t+s} \frac{(1+\rho)}{(1-\pi)(1+g_{t+s})^{-\alpha} + \pi \int_{g_d}^{g_u} (1+g_{t+s})^{-\alpha} dG(g_{t+s})}. \quad \text{(A14)}$$

In addition, we know from the Euler condition that the pricing kernel must be such that:

$$\mathrm{E}_t\left[\beta \left(\frac{D_{t+1}}{D_t}\right)^{-\alpha} \frac{(1+\rho)}{(1-\pi)(1+g_{t+k})^{-\alpha} + \pi \int_{g_d}^{g_u} (1+g_{t+k})^{-\alpha} dG(g_{t+k})} \right] = 1. \quad \text{(A15)}$$

Using equation (A15) and adding $D_{t+k}^{CI^*}$ to both sides of equation (A12), we obtain:

$$S_{t+k}^{CI^*} + D_{t+k}^*$$
$$= \mathrm{E}_{t+k}\left[\beta\left(\frac{D_{t+\mathrm{k}+1}}{D_{t+k}}\right)^{-\alpha}\frac{(1+\rho)}{(1-\pi)(1+g_{t+k})^{-\alpha}+\pi\int_{g_d}^{g_u}(1+g_{t+k})^{-\alpha}dG(g_{t+k})}(S_{t+k+1}^{CI^*}\right. \quad \text{(A16)}$$
$$\left.+ D_{t+k+1}^*)\right].$$

This shows that $(S_{t+k}^{CI^*} + D_{t+k}^*)$ follows a martingale under this conditional probability measure so that the risk-neutral density is:

$$\hat{p}_t(S_{t+k}^{CI})$$
$$= \beta\left(\frac{D_{t+1}}{D_t}\right)^{-\alpha}\frac{(1+\rho)}{(1-\pi)(1+g_{t+k})^{-\alpha}+\pi\int_{g_d}^{g_u}(1+g_{t+k})^{-\alpha}dG(g_{t+k})}p_t(D_{t+k}). \quad \text{(A17)}$$

Consequently, the one-period state-price density can be written as:

$$\tilde{p}_t(S_{t+k}^{CI}) = \beta\left(\frac{D_{t+\mathrm{k}}}{D_t}\right)^{-\alpha}\frac{1}{1+r_{t+k}^{CI}}$$
$$\cdot\frac{(1+\rho)}{(1-\pi)(1+g_{t+k})^{-\alpha}+\pi\int_{g_d}^{g_u}(1+g_{t+k})^{-\alpha}dG(g_{t+k})}p_t(D_{t+k}) \quad \text{(A18)}$$
$$= \beta\left(\frac{D_{t+1}}{D_t}\right)^{-\alpha}p_t(D_{t+k})$$

where r_{t+k}^{CI} is the one-period risk-free interest rate. Additionally, Pliska (1997) shows that if the risk-neutral measure on a single period model is unique and exists, this is a sufficient condition to have a unique risk-neutral measure on an infinite period model obtained as a repetition of many static, single-period models. In our case, the infinite period model risk-neutral measure can be obtained using the independence of breaks on the mean dividend growth rates and by taking all paths that could guide to a particular state in $t+\tau$ periods. In this context, $p_t^{CI}(S_{t+\tau}^{CI})$ is the state price density of all paths that lead to the state in which the dividend is $D_{t+\tau}$, while the expected value of $D_{t+\tau}$ is:

$$\mathrm{E_t}[D_{t+\tau}] = D_t\mathrm{E_t}\left[\frac{D_{t+1}}{D_t}\mathrm{E}_{t+1}\left[\left(\frac{D_{t+2}}{D_{t+1}}\right)\ldots\mathrm{E}_{t+\tau-1}\left[\left(\frac{D_{t+\tau}}{D_{t+\tau-1}}\right)\right]\right]\right]. \quad \text{(A19)}$$

Furthermore, using the independence of $\{\varepsilon_{t+i}\}_{i=1}^{\tau}$ and $\{g_{t+i-1}\}_{i=1}^{\tau}$ we have:

$$\mathrm{E_t}[D_{t+\tau}] = D_t\mathrm{E_t}\left[\exp\left(\sqrt{\tau}\sigma\varepsilon_{t+\tau} - \tau\sigma^2/2\right)\prod_{i=1}^{\tau}(1+g_{t+i-1})\right]. \quad \text{(A20)}$$

At this point, let z be the number of breaks between t and $t+\tau$; this is a random variable drawn from a Binomial distribution, $\varphi(z|\tau,\pi)$, with parameters τ and π; $\{h_i\}_{i=0}^{z}$ are the time periods

between breaks which are also random variables that follow geometric distributions with parameter π, $\eta(h_i|\pi)$, where $\tau = \sum_{i=0}^{z} h_i$. Then, on each path:

$$D_{t+\tau}^{CI} = D_t \exp\left(\sqrt{\tau}\sigma\varepsilon_{t+\tau} - \tau\sigma^2/2\right) \cdot \prod_{i=1}^{z+1}(1 + g_{t+v_{i-1}})^{h_i} \qquad \text{(A21)}$$

where $\{g_{t+h_i}\}_{i=1}^{z}$ are drawn from a univariate density $g_{t+h_{i-1}} \sim G(\cdot)$ and pdf $\varrho(g_{t+h_i})$ defined on the support $[g_d, g_u]$, while $g_{t+h_0} = g_t$ and $g_{t+\tau} = g_{t+h_z}$. Consequently,

$$p_t(D_{t+k}) = \phi(\varepsilon_{t+\tau}|0,\sigma)\varphi(z|\tau,\pi)\eta(h_0|\pi)\left(\eta(h_1|\pi)\varrho\left(g_{t+h_1}\right) \cdot \ldots \cdot \eta(h_z|\pi)\varrho\left(g_{t+h_z}\right)\right) \quad \text{(A22)}$$

and thus from equation (A18), we have:

$$\tilde{p}_t(S_{t+k}^{CI}) = \beta^{\tau}\left(\frac{D_{t+\tau}}{D_t}\right)^{-\alpha}\phi(\varepsilon_{t+\tau}|0,\sigma)\varphi(z|\tau,\pi)\eta(h_0|\pi)\left(\eta(h_1|\pi)\varrho\left(g_{t+h_1}\right) \cdot \eta(h_z|\pi)\varrho\left(g_{t+h_z}\right)\right). \qquad \text{(A23)} \ \square$$

Appendix B: Chu, Stinchcombe and White's Real Time Breakpoint Test

We use the test introduced by Chu *et al.* (1996) to estimate the probability of breaks in the mean dividend growth rate. Chu *et al.* (1996) present a dynamic test for structural breaks through which market participants can identify a real time shift in the (conditional) mean function. Consider the dividend random walk process in equation (1). Let v be the minimum number of periods over which the drift is assumed to be constant, given that n is the number of periods from the most recent break (i.e. $\mu_{t-n+1} = \mu_{t-n+2} = \ldots = \mu_{t-n+v}$). Assuming that the representative agent starts detecting the presence of breaks after a period v, Chu *et al.* (1996) propose the use of the following *fluctuation detector* in the case of a univariate location (mean function) model:

$$\hat{Z}_t = n\hat{s}_0^{-1}(\hat{\mu}_t - \hat{\mu}_v) \qquad \text{(B1)}$$

where $\hat{\mu}_t$ and $\hat{\mu}_v$ are the parameter estimates at time t and v. We defined $\boldsymbol{\xi}_t$ as the vector of signals about μ_t in equation (10); therefore $\hat{\mu}_t = \bar{\xi}_t = (1/n)\sum_{i=t-n+1}^{t}\xi_i$ and $\hat{\mu}_v = \bar{\xi}_v = (1/v)\sum_{i=t-n+1}^{t-n+v}\xi_i$, while $\hat{s}_0 = (v^{-1}\sum_{i=t-n+1}^{t-n+v}(\xi_i - \hat{\mu}_v)^2)^{0.5}$. Under the null hypothesis of no breaks, Chu *et al.* (1996) report asymptotic bounds for the statistic $|\hat{Z}_t|$:

$$\lim_{v\to\infty} P\left\{|\hat{Z}_t| \geq \sqrt{v}\left(\frac{n-v}{v}\right)\left[\left(\frac{n}{n-v}\right)\left[a^2 + \ln\left(\frac{n}{n-v}\right)\right]\right]^{\frac{1}{2}}\right\} \cong 2\left(1 - \Phi(a) + a\phi(a)\right). \qquad \text{(B2)}$$

Here $\Phi(\cdot)$ and $\phi(\cdot)$ are the cdf and pdf of a standard normal random variable, respectively, while a is a constant related to the chosen significance level of the test. The intuition behind this test is that given a significance level, an agent could start the calculation of $\hat{Z}_t$ recursively and in real-time after

v signals received from the previous break to detect a new one. The testing process starts again after the detection of the new break. In this paper we assume that dividends are paid out daily, which is true for many market indexes. For that reason and with the objective of detecting breaks, we use daily dividend time series for the S&P 500 index between 1996 and 2007 which are de-seasonalized and adjusted by the consumer price index. We set v=125 which represents six months of trading, and we use a 5% significance. We detect eight breaks in the period between 1996 and 2007. Figure B1 shows the breaks detected in the sample period.

[Insert Figure B1 here]

Appendix C: Option Data Used in the Paper

We use data from the U.S. option market over the period 1996 - 2007 to estimate a few typical indicators concerning the shape and dynamics of the IVS to be compared to the results obtained from the simulations of calibrated versions of our incomplete information, Bayesian learning framework. We include individual call equity options and call S&P 500 index options which are American and European style, respectively. We obtain the data from the OptionMetrics database that reports daily closing bid and ask quotes, BS implied volatilities, maturities, strike prices, synchronous (after appropriate adjustments that employ the put-call parity) closing underlying stock (index) prices, and the risk-free term-structure of interest rates. Option prices correspond to closing bid-ask midpoints. In relation to single-name stock options, we select only options in which the underlying stocks pay dividends, to ensure the realism of our model. We choose the 150 names with the highest volume which have been continuously traded over our sample period.[30] We sample option market data only on Wednesdays, in a similar way to our simulations. We apply four exclusionary criteria in order to filter out observations that represent noisy data, possibly recording errors, and that can hardly be thought to be expressions of well-functioning markets. First, we eliminate all observations that violate basic no-arbitrage bounds, such as European put-call parity, American put-call boundaries, the lower bound etc. (see Bernales and Guidolin, 2012, for a complete list of restrictions that are applied as filters). Second, we delete all contracts with less than six trading days and more than one year to expiration as their prices are usually noisy. Third and similar to Gonçalves and Guidolin (2006), we exclude contracts with prices lower than \$0.30 for equity options and \$3/8 for S&P 500 index options to avoid the effects of price

[30] The full list of 150 option series is available from the authors upon request.

discreteness on implied volatilities (note that in the case of equity options the minimum tick is \$0.05 for trading prices lower than \$3, while for index options the smallest tick is \$1/16). Fourth, following Dumas *et al.* (1998), we exclude options contracts for which the moneyness is either less than 0.90 or in excess of 1.10, because deep in- and out-of-the money option contracts could cause additional noise in the analyses and option series beyond these thresholds are normally illiquid and infrequently traded.

Appendix D: Additional Calibration Experiments and Robustness Checks

In this appendix, we report simulation results from additional parameter set ups. Table D1 shows summary statistics for simulated real dividends, default risk-free interest rates, stock prices, and short-term at-the-money option contract prices, and their BS IVs. As in the case of Table I, D1 presents averages over sets of 1,000 simulations over a range of parameter combinations under three scenarios: no breaks; breaks and complete information; breaks and incomplete information with learning. In the initial two panels of Table D1 we set the coefficient of relative risk aversion at 0.5, while in the third and fourth panels we set it at 5.0. Otherwise, each pair of panels reports first results for the case of low volatility of fundamentals (σ = 5%) and the case of high volatility (σ = 30%). In table D1, the case of α = 0.5 confirms the qualitative remarks expressed in Section 3.2 with reference to the effects of learning on average IVs, although the effects are now weaker, especially in the case in which σ = 5%. When the CRRA is instead set to 5, both the equilibrium riskless rates and the resulting approximate ATM 1-month to maturity IVs appear to be absurdly high, especially in the case of σ = 30%. As commented in Section 3.2 this is an effect not of rational learning, but of sheer aversion to risk. All in all, while results appear to be robust to the use of any α well below 1, the same cannot be said for levels of risk aversion in excess of 2-3. Because, under power utility $\alpha \leq$ 0.5 is consistent with estimated elasticities of intertemporal substitution in excess of 2, this finding seems realistic.

Table D2 shows instead the dynamic features of the level, slopes, and curvatures of the IVS in an economy under breaks and incomplete information with learning for the same four alternative parameterization that appear in Table D1. Therefore Table D2 should be compared with Table III in the main body of the paper. Also in this case, results are qualitatively similar (in fact, occasionally closer to the empirical estimates in Table III) to those in Table II when α = 0.5. However, they are often excessive or simply unrealistic when compared to Table III when α = 5. This means that high CRRA does no good to the accuracy or the realism of our results and that in fact, high risk aversion—when combined with Bayesian learning—ends up missing central properties of the dynamics of the IVS. Finally, Table D3 reports estimates of the simulated cross-sectional

relationships of the IVS shape features also in an economy under breaks and incomplete information with learning. The results are largely similar to the ones reported above.

[Insert Table D1 here]

[Insert Table D2 here]

[Insert Table D3 here]

Appendix E: Calibrating the Fit of Deterministic IVS Models

In this appendix, we report the estimated fit of a simple and yet popular deterministic IVS model proposed in Dumas *et al.* (1998), using implied volatilities simulated from a calibrated economy under breaks and incomplete information with learning. The implied volatility polynomial function that has been estimated is:

$$IV(Mon,\tau) = b_0 + b_1 Mon + b_2 Mon^2 + b_3\left(\frac{\tau}{365}\right) + b_4\left(\frac{\tau}{365}\right)^2 + b_5 Mon\left(\frac{\tau}{365}\right) + \epsilon \quad \text{(E1)}$$

where $IV(Mon,\tau)$ is the implied volatility of a call option contract with moneyness Mon and time-to-maturity τ. Table E1 presents the coefficient estimates obtained by OLS and overall measures of fit for two alternative calibrations (high and low σ) and three alternative values for α. The coefficients are to be compared to the empirical ones estimated from data on S&P 500 index calls or the average across 150 deterministic IVS regressions estimated for each of the stock options detailed in Appendix C. Table E1 shows that the *IVS* generated by the Bayesian learning model can be characterised by an implied volatility polynomial function as in Dumas *et al.* (1998) in a similar way to the implied volatilities reported in option trading data.

[Insert Table E1 here]

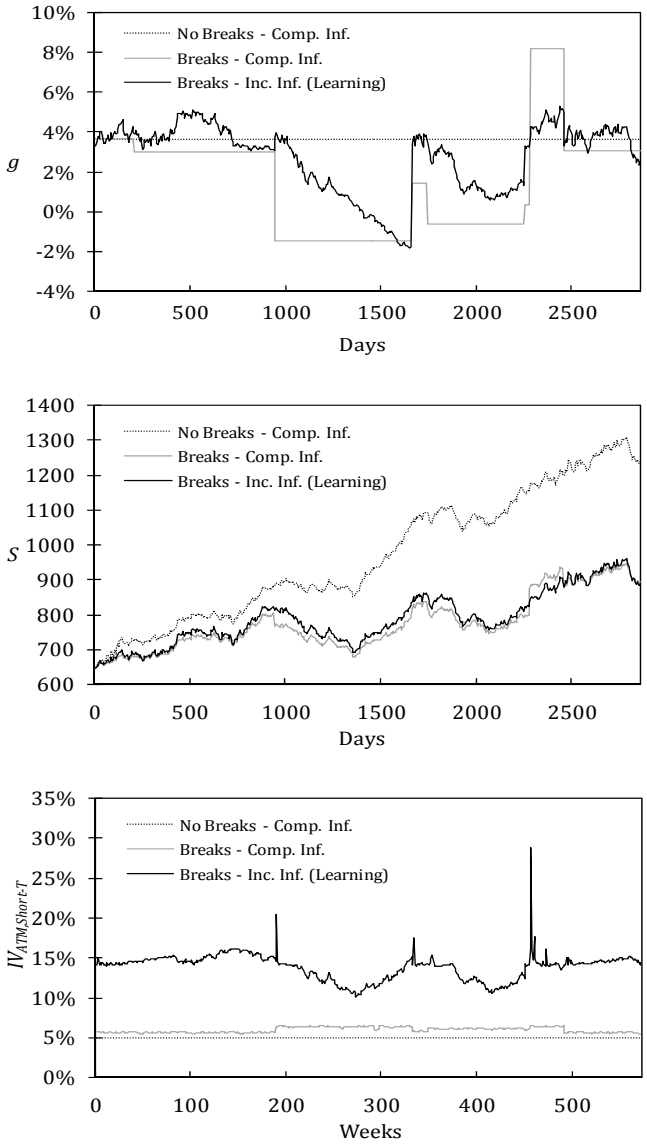

Figure 1. Evolutions of mean dividend growth rates, stock prices, and at-the-money short-term IVs under three scenarios on investor's expectations. The figure shows the outcome for one simulated path concerning the dynamics over a 12-year sample for the mean dividend growth rate (g), stock prices (S), and at-the-money short-term IVs ($IV_{ATM,Short\text{-}T}$) under three scenarios: no breaks; breaks and complete information; and breaks and incomplete information with rational learning. $IV_{ATM,Short\text{-}T}$ is the implied volatility corresponding to a call option contract with 30-days to the expiration date (calendar days) and at-the-money. Given that the simulations replicate option prices according to CBOE rules, we calculate $Call_{ATM,Short\text{-}T}$ by linear interpolation using the four contracts around the 30-days time-to-maturity and with closest strike price to S. The assumed parameters are: α=0.2; π=0.00301; ρ=8.9%; σ=5.0%; g_u=8.8%; and g_u=-1.5%.

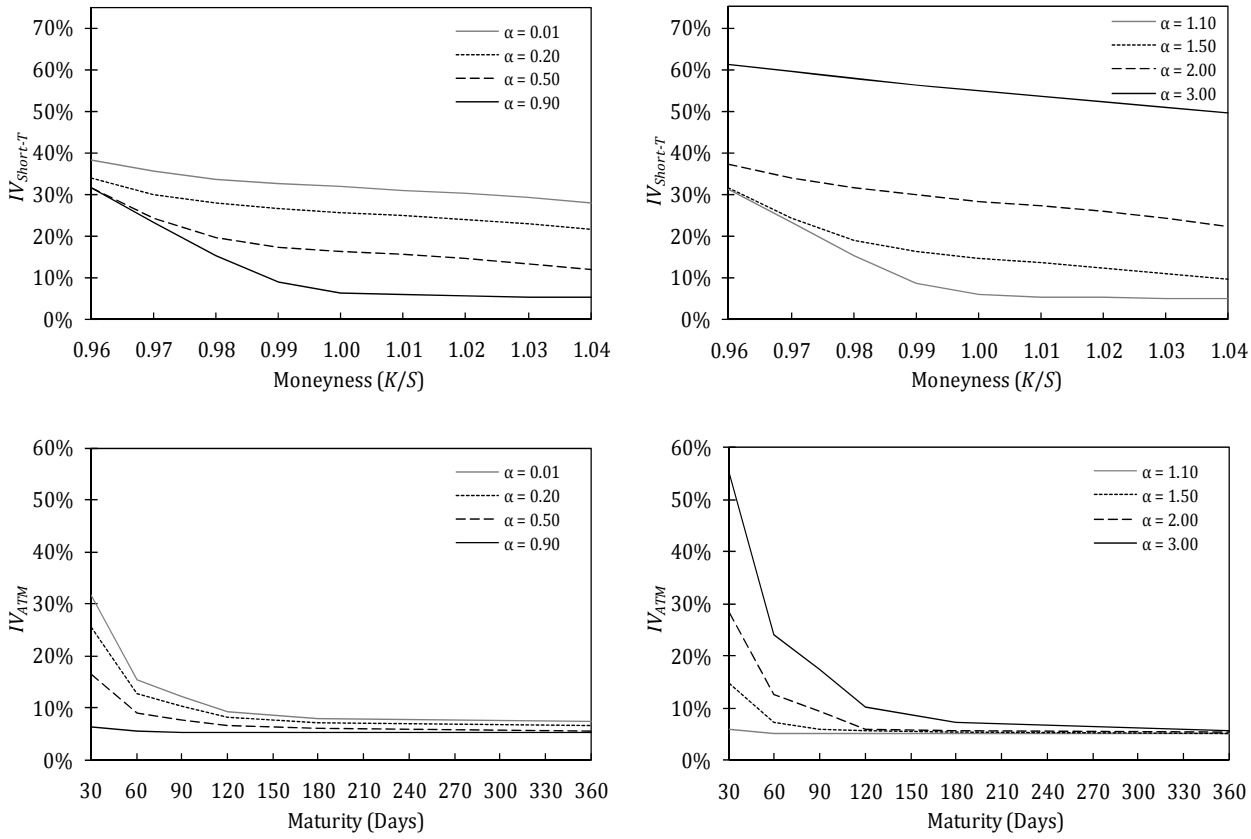

Figure 2. Sensitivity analysis on the average behaviour of the implied volatility surface one month after a break in an economy with learning using alternative CRRA levels. The figure presents the average behaviour, *one month* after a break in g_t, of implied volatilities in an economy under breaks and incomplete information with learning. This figure shows implied volatilities as a function of moneyness using short-term option contracts (upper windows) and implied volatilities as a function of time-to- maturity using at-the money option contracts (lower windows). $IV_{Short\text{-}T}$ (IV_{ATM}) represents the implied volatilities corresponding to call option contracts with 30-days to the expiration date (strike prices equal to S). Given that the simulations replicate option prices according to CBOE rules, we calculate $Call_{ATM,Short\text{-}T}$ by simple linear interpolation using the four contracts around the 30-days time-to-maturity and with closest strike price to S. The assumed parameters are: π=0.00301; ρ=8.9%; σ=5.0%; g_u=8.8%; and g_u=-1.5%.

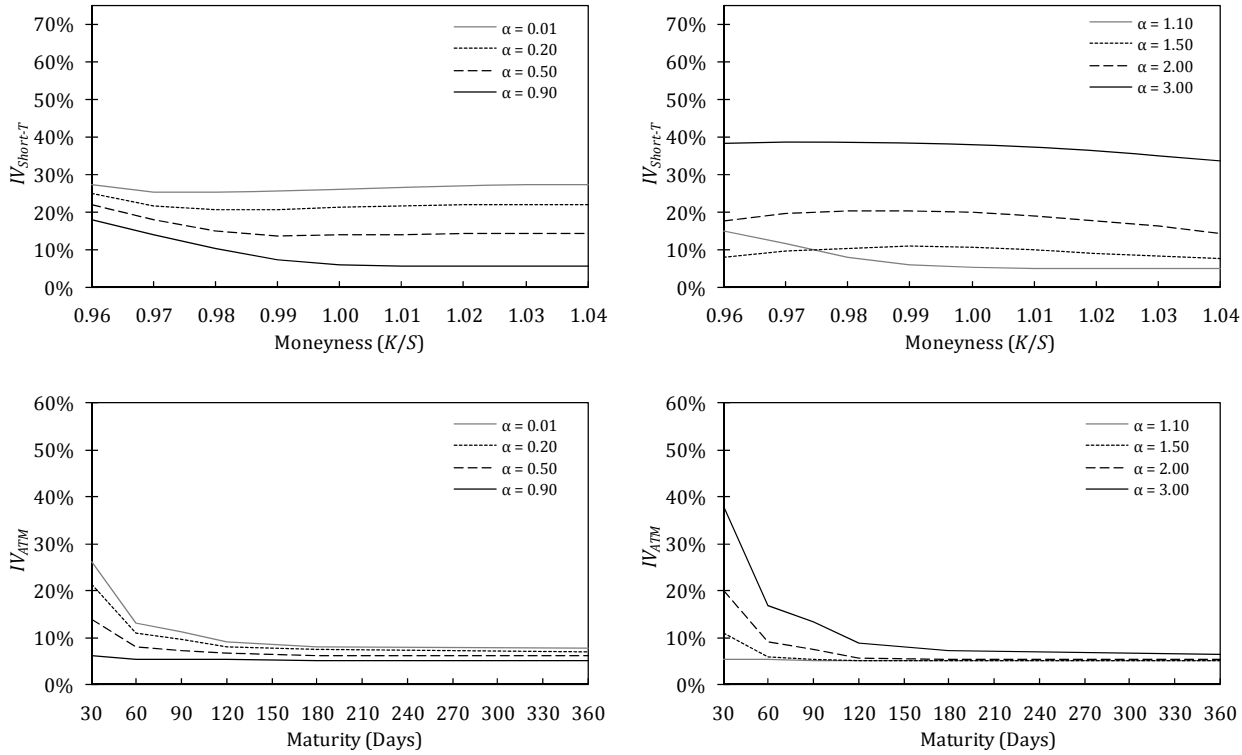

Figure 3. Sensitivity analysis on the average behaviour of the implied volatility surface one month after a break in an economy with learning using alternative CRRA levels. The figure presents the average behaviour, *one year* after a break in g_t, of implied volatilities in an economy under breaks and incomplete information with learning. This figure shows implied volatilities as a function of moneyness using short-term option contracts (upper windows) and implied volatilities as a function of time-to- maturity using at-the money option contracts (lower windows). The assumed parameters are: π=0.00301; ρ=8.9%; σ=5.0%; g_u=8.8%; and g_u=-1.5%.

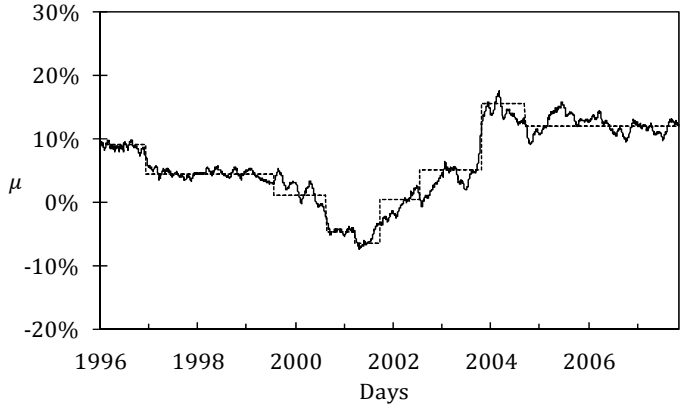

Figure B1. Structural breaks affecting the drift of the random walk process in equation (1). The solid line represents the recursive mean dividend growth rate (the drift) estimated with a rolling window of 125 trading days using continuously compounded dividends on the S&P 500 index, de-seasonalized and adjusted by the consumer price index to obtain real dividends, between 1996 and 2007. The dotted line shows structural breaks estimated for the conditional mean function of dividends. Breaks were detected in correspondence of December 1996, August 1999, September 2000, April 2001, October 2001, August 2002, November 2003, and October 2004.

Table I

Simulation Summary under Three Alternative Scenarios for Investor's Expectations

The variables g, S, and $IV_{ATM,Short\text{-}T}$ are defined in Figure 1. Div is the daily dividend simulated while $r_{f,1\ day}$ is the one-day risk-free interest rate. $Call_{ATM,Short\text{-}T}$ is the price of a call option contract with 30-days to the expiration date (calendar days) and at-the-money. Given that the simulations replicate option prices according to CBOE rules, we calculate $Call_{ATM,Short\text{-}T}$ by simple linear interpolation using the four contracts around the 30-days time-to-maturity and with closest strike price to S.

Scenario	Variable	Mean	Median	Std. Dev.	Skewness	Excess Kurtosis	Min.	Max.
			α=0.2					
		π=66.7%, ρ=8.9%, σ=5.0%, g_u=8.8%, and g_d=-1.5%						
No Breaks - Comp. Inf.	Div	0.17	0.17	0.03	1.12	1.74	0.10	0.37
	g	3.65%	3.65%	0.00%	NA	NA	3.65%	3.65%
	$r_{f,1\ day}$	9.68%	9.68%	0.00%	NA	NA	9.68%	9.68%
	S	813.22	761.05	153.29	1.12	1.74	109.43	1301.20
	$Call_{ATM,Short\text{-}T}$	4.39	4.30	1.57	0.38	-0.07	1.01	11.95
	$IV_{ATM,Short\text{-}T}$	5.00%	5.00%	0.00%	NA	NA	5.00%	5.00%
Breaks - Comp. Inf.	Div	0.18	0.17	0.04	1.28	1.92	0.11	0.38
	g	3.66%	3.65%	2.96%	0.00	-1.21	-1.49%	8.78%
	$r_{f,1\ day}$	9.67%	9.75%	0.53%	-0.05	-0.90	9.29%	10.01%
	S	814.27	768.34	174.55	1.23	1.69	446.67	1678.97
	$Call_{ATM,Short\text{-}T}$	5.42	5.21	2.08	0.66	0.97	1.02	16.81
	$IV_{ATM,Short\text{-}T}$	5.75%	5.82%	0.31%	0.76	0.01	5.10%	7.44%
Breaks - Inc. Inf. (Learning)	Div	0.18	0.17	0.04	1.28	1.92	0.11	0.38
	g	3.64%	3.60%	1.62%	0.08	-0.16	-0.52%	8.33%
	$r_{f,1\ day}$	9.67%	9.56%	0.29%	0.04	-0.15	9.31%	10.03%
	S	814.10	769.82	173.25	1.25	1.84	449.06	1730.23
	$Call_{ATM,Short\text{-}T}$	12.75	12.34	3.12	1.24	9.53	2.93	91.95
	$IV_{ATM,Short\text{-}T}$	19.24%	19.62%	3.60%	0.93	3.23	7.13%	74.11%

Scenario	Variable	Mean	Median	Std. Dev.	Skewness	Excess Kurtosis	Min.	Max.
			α=0.2					
		π=66.7%, ρ=9.6%, σ=30.0%, g_u=9.5%, and g_d=-5.0%						
No Breaks - Comp. Inf.	Div	0.18	0.13	0.16	2.46	8.97	0.00	1.64
	g	2.25%	2.25%	0.00%	NA	NA	2.25%	2.25%
	$r_{f,1\ day}$	10.09%	10.09%	0.00%	NA	NA	10.09%	10.09%
	S	698.66	501.26	626.41	2.46	9.07	18.47	6023.90
	$Call_{ATM,Short\text{-}T}$	18.32	13.93	12.83	0.80	-0.17	0.13	210.41
	$IV_{ATM,Short\text{-}T}$	30.00%	30.00%	0.00%	NA	NA	30.00%	30.00%
Breaks - Comp. Inf.	Div	0.18	0.13	0.17	2.56	9.07	0.00	1.66
	g	2.27%	2.25%	4.17%	0.01	-1.19	-4.94%	9.48%
	$r_{f,1\ day}$	10.08%	10.11%	0.79%	-0.09	-0.95	9.52%	10.52%
	S	700.93	504.80	676.20	2.62	9.67	18.91	6797.87
	$Call_{ATM,Short\text{-}T}$	26.13	23.30	18.44	1.28	2.35	1.60	241.42
	$IV_{ATM,Short\text{-}T}$	31.63%	31.28%	0.83%	0.83	0.77	30.06%	33.20%
Breaks - Inc. Inf. (Learning)	Div	0.18	0.13	0.17	2.56	9.07	0.00	1.66
	g	2.24%	2.22%	2.68%	0.25	-0.35	-1.73%	9.23%
	$r_{f,1\ day}$	10.04%	10.04%	0.13%	0.21	-0.31	9.79%	10.55%
	S	699.91	503.95	673.46	2.60	9.34	19.96	6990.88
	$Call_{ATM,Short\text{-}T}$	35.13	34.71	22.62	3.36	15.78	1.74	424.78
	$IV_{ATM,Short\text{-}T}$	43.28%	42.19%	5.40%	4.23	9.15	30.79%	221.23%

Table II
Simulated Properties of the Implied Volatility Surface under Rational Learning

The table contains time series statistics concerning the level, slope, and curvature of the IVS in both the moneyness and maturity dimensions in an economy under breaks and incomplete information with learning. The table shows average simulation outcomes using two parameter set ups. $IV_{ATM,Short\text{-}T}$ is defined in Figure 1. We define $Slope_{Mon}$ ($Slope_{Mat}$) as the average across simulation trials of numerical first derivatives with respect to moneyness (time to maturity) computed from all the pairs of priced options with neighbouring moneyness levels and 30 days to maturity (neighbouring maturity levels and closest at-the-money). In addition, $Curv_{Mon}$ ($Curve_{Mat}$) is the average across simulation trials of numerical second derivatives with respect to moneyness (time to maturity) computed from all triplets of priced options with neighbouring moneyness levels and 30 days to maturity (neighbouring maturity levels and closest at-the-money). Serial Correlation refers to a Box-Pierce test applied to the first-order Ljung-Box statistic. The ARCH(1) and ARCH(3) statistics are the values of the LM test for ARCH effects using one and three lags, respectively. The percentage of simulations with significant statistics at a 10% size for the associated test statistics are reported in parentheses.

Variable	Mean	Std. Dev.	Skewness	Excess Kurtosis	Serial Correlation	ARCH(1)	ARCH(3)
				α=0.2			
	Panel A: π=66.7%, ρ=8.9%, σ=5.0%, g_u=8.8%, and g_d=-1.5%						
$IV_{ATM,Short\text{-}T}$	19.24%	3.60%	0.93	3.23	55.83	41.05	42.57
					(98.80)	(91.30)	(91.10)
$Slope_{Mon}$	-0.35	0.14	-0.31	2.35	18.04	5.66	10.10
					(78.50)	(39.30)	(42.70)
$Curv_{Mon}$	30.90	20.99	0.13	11.62	12.80	4.04	7.60
					(62.20)	(28.20)	(29.40)
$Slope_{Mat}$	-0.31	0.08	-0.02	1.81	53.16	37.03	38.76
					(98.80)	(87.50)	(86.00)
$Curv_{Mat}$	3.28	1.12	0.21	4.47	47.56	29.66	31.61
					(98.80)	(84.80)	(81.90)
	Panel B: π=66.7%, ρ=9.6%, σ=30.0%, g_u=9.5%, and g_d=-5.0%						
$IV_{ATM,Short\text{-}T}$	43.28%	5.40%	4.23	9.15	50.46	39.74	38.31
					(93.30)	(88.70)	(90.30)
$Slope_{Mon}$	-0.19	0.15	-0.57	7.54	16.07	4.41	8.89
					(75.80)	(31.90)	(35.30)
$Curv_{Mon}$	2.87	2.40	0.44	17.60	9.37	2.86	7.23
					(53.40)	(27.80)	(26.20)
$Slope_{Mat}$	-0.31	0.09	-0.03	3.14	49.85	33.87	36.65
					(92.20)	(78.90)	(79.20)
$Curv_{Mat}$	3.53	1.72	0.62	6.38	44.38	27.61	26.48
					(92.20)	(77.90)	(78.30)

Table III

Empirical Properties of the Implied Volatility Surface Using Options Market Data

The table contains time series statistics concerning the level, slope, and curvature of the IVS in both the moneyness and maturity dimensions computed from U.S. option market data over the period 1997 - 2007. Panel A (Panel B) reports statistics for IVS shape features using S&P 500 index options (150 individual equity options on dividend-paying stocks). The options market data are introduced in Appendix C. $IV_{ATM,Short\text{-}T}$ is defined in Figure 1, while $Slope_{Mon}$, $Curv_{Mon}$, $Slope_{Mat}$, and $Curv_{Mon}$ are defined in Table II. Serial Correlation refers to a Box-Pierce test applied to the first-order Ljung-Box statistic. The ARCH(1) and ARCH(3) statistics are the values of the LM test for ARCH effects using one and three lags, respectively. The percentage of option series with significant statistics at a 10% size for the associated test statistics are reported in parentheses. Because in panel A only the S&P 500 index option series is used in the tests, in this case the percentage in parenthesis is simply 0 or 100.

Variable	Mean	Std. Dev.	Skewness	Excess Kurtosis	Serial Correlation	ARCH(1)	ARCH(3)
	Panel A: S&P 500 Options						
$IV_{ATM,Short\text{-}T}$	16.65%	5.90%	0.71	0.42	422.82	266.05	267.56
					(100.00)	(100.00)	(100.00)
$Slope_{Mon}$	-0.64	0.21	-0.48	0.69	82.70	15.21	18.21
					(100.00)	(100.00)	(100.00)
$Curv_{Mon}$	13.84	14.40	0.08	7.38	14.02	0.35	15.42
					(100.00)	(0.00)	(100.00)
$Slope_{Mat}$	0.03	0.07	-0.60	2.48	205.68	126.97	141.14
					(100.00)	(100.00)	(100.00)
$Curv_{Mat}$	-0.12	0.60	0.24	5.06	23.02	0.18	36.69
					(100.00)	(0.00)	(100.00)
	Panel B: Equity Options						
$IV_{ATM,Short\text{-}T}$	40.34%	5.63%	0.67	0.86	59.33	29.06	31.39
					(98.00)	(74.00)	(69.33)
$Slope_{Mon}$	-0.21	0.70	1.03	26.31	4.72	2.18	7.02
					(32.67)	(13.33)	(17.33)
$Curv_{Mon}$	2.62	10.61	-0.35	11.50	1.85	2.64	4.98
					(18.67)	(15.33)	(18.67)
$Slope_{Mat}$	-0.04	0.09	-0.90	2.82	36.23	12.44	14.94
					(96.00)	(60.00)	(57.33)
$Curv_{Mat}$	0.08	0.55	0.59	3.92	17.39	7.38	10.40
					(90.00)	(48.67)	(44.67)

Table IV
Cross-Sectional Relationships of IVS Features under Rational Learning

The table contains correlations for the level, slope, and curvature of the IVS in both the moneyness and maturity dimensions in an economy under breaks and incomplete information with learning. The table shows average simulation outcomes using two parameter set ups. $IV_{ATM,Short\text{-}T}$ is defined in Figure 1, while $Slope_{Mon}$, $Curv_{Mon}$, $Slope_{Mat}$, and $Curv_{Mon}$ are defined in Table II. The percentage of simulations with significant statistics at a 10% size for the associated test statistics are reported in parentheses.

Variable	$IV_{ATM,Short\text{-}T}$	$Slope_{Mon}$	$Curv_{Mon}$	$Slope_{Mat}$	$Curv_{Mat}$
			α=0.2		
	Panel A: π=66.7%, ρ=8.9%, σ=5.0%, g_u=8.8%, and g_d=-1.5%				
$IV_{ATM,Short\text{-}T}$	1.00				
	(100.00)				
$Slope_{Mon}$	-0.38	1.00			
	(80.10)	(100.00)			
$Curv_{Mon}$	-0.14	-0.47	1.00		
	(67.90)	(81.30)	(100.00)		
$Slope_{Mat}$	-0.96	0.32	0.17	1.00	
	(99.20)	(76.40)	(64.50)	(100.00)	
$Curv_{Mat}$	0.89	-0.28	-0.15	-0.91	1.00
	(98.90)	(74.80)	(70.30)	(98.50)	(100.00)
	Panel B: π=66.7%, ρ=9.6%, σ=30.0%, g_u=9.5%, and g_d=-5.0%				
$IV_{ATM,Short\text{-}T}$	1.00				
	(100.00)				
$Slope_{Mon}$	-0.35	1.00			
	(74.60)	(100.00)			
$Curv_{Mon}$	-0.12	-0.46	1.00		
	(66.90)	(79.70)	(100.00)		
$Slope_{Mat}$	-0.42	0.31	0.00	1.00	
	(89.90)	(72.40)	(58.90)	(100.00)	
$Curv_{Mat}$	0.38	-0.11	-0.09	-0.72	1.00
	(79.70)	(54.60)	(52.80)	(81.20)	(100.00)

Table V

Empirical Cross-Sectional Relationships of IVS Features Using Options Market Data

The table contains correlations for the level, slope, and curvature of the IVS in both the moneyness and maturity dimensions computed from U.S. option market data over the period 1997 - 2007. Panel A (Panel B) reports statistics for IVS shape features using S&P 500 index options (150 individual equity options on dividend-paying stocks). The options market data are introduced in Appendix C. $IV_{ATM,Short\text{-}T}$ is defined in Figure 1, while $Slope_{Mon}$, $Curv_{Mon}$, $Slope_{Mat}$, and $Curv_{Mon}$ are defined in Table II. The percentage of option series with significant statistics at a 10% size for the associated test statistics are reported in parentheses.

Variable	$IV_{ATM,Short\text{-}T}$	$Slope_{Mon}$	$Curv_{Mon}$	$Slope_{Mat}$	$Curv_{Mat}$
	Panel A: S&P 500 Options				
$IV_{ATM,Short\text{-}T}$	1.00				
	(100.00)				
$Slope_{Mon}$	-0.24	1.00			
	(100.00)	(100.00)			
$Curv_{Mon}$	-0.35	-0.09	1.00		
	(100.00)	(100.00)	(100.00)		
$Slope_{Mat}$	-0.40	0.00	0.27	1.00	
	(100.00)	(0.00)	(100.00)	(100.00)	
$Curv_{Mat}$	0.02	0.07	-0.05	-0.29	1.00
	(0.00)	(0.00)	(0.00)	(100.00)	(100.00)
	Panel B: Equity Options				
$IV_{ATM,Short\text{-}T}$	1.00				
	(100.00)				
$Slope_{Mon}$	-0.11	1.00			
	(46.67)	(100.00)			
$Curv_{Mon}$	-0.29	-0.11	1.00		
	(86.00)	(64.67)	(100.00)		
$Slope_{Mat}$	-0.57	0.28	0.06	1.00	
	(97.33)	(80.00)	(46.67)	(100.00)	
$Curv_{Mat}$	0.24	-0.25	0.03	-0.62	1.00
	(76.67)	(80.00)	(41.33)	(99.33)	(100.00)

Table D1

Simulation Summary under Six Alternative Scenarios for Investor's Expectations

The variables g, S, and $IV_{ATM,Short\text{-}T}$ are defined in Figure 1. *Div* is the daily dividend simulated while $r_{f,1\ day}$ is the one-day risk-free interest rate. $Call_{ATM,Short\text{-}T}$ is the price of a call option contract with 30-days to the expiration date (calendar days) and at-the-money. Given that the simulations replicate option prices according to CBOE rules, we calculate $Call_{ATM,Short\text{-}T}$ by simple linear interpolation using the four contracts around the 30-days time-to-maturity and with closest strike price to S.

Scenario	Variable	Mean	Median	Std. Dev.	Skewness	Excess Kurtosis	Min.	Max.
			α=0.5					
		π=66.7%, ρ=8.9%, σ=5.0%, g_u=8.8%, and g_d=-1.5%						
No Breaks - Comp. Inf.	*Div*	0.17	0.17	0.03	1.12	1.74	0.10	0.37
	g	3.65%	3.65%	0.00%	NA	NA	3.65%	3.65%
	$r_{f,\,1\,day}$	10.87%	10.87%	0.00%	NA	NA	10.87%	10.87%
	S	677.92	630.32	129.27	1.12	1.74	98.31	1093.35
	$Call_{ATM,Short\text{-}T}$	3.73	3.64	1.38	0.34	-0.13	0.55	11.94
	$IV_{ATM,Short\text{-}T}$	5.00%	5.00%	0.00%	NA	NA	5.00%	5.00%
Breaks - Comp. Inf.	*Div*	0.18	0.17	0.04	1.28	1.92	0.11	0.38
	g	3.66%	3.65%	2.96%	0.00	-1.21	-1.49%	8.78%
	$r_{f,\,1\,day}$	10.88%	10.87%	1.32%	-0.06	-0.91	9.91%	11.66%
	S	683.44	645.19	143.97	1.25	1.77	382.30	1406.32
	$Call_{ATM,Short\text{-}T}$	4.53	4.32	1.80	0.69	0.59	0.68	13.49
	$IV_{ATM,Short\text{-}T}$	5.43%	5.58%	0.20%	0.64	0.87	5.04%	6.75%
Breaks - Inc. Inf. (Learning)	*Div*	0.18	0.17	0.04	1.28	1.92	0.11	0.38
	g	3.64%	3.60%	1.48%	0.08	-0.16	-0.52%	8.33%
	$r_{f,\,1\,day}$	10.86%	10.84%	0.72%	0.04	-0.17	10.08%	11.54%
	S	683.34	646.44	143.54	1.26	1.87	383.56	1437.51
	$Call_{ATM,Short\text{-}T}$	7.51	7.27	2.06	1.53	17.21	1.38	68.29
	$IV_{ATM,Short\text{-}T}$	13.91%	13.57%	2.53%	1.73	14.13	6.07%	56.78%
Scenario	Variable	Mean	Median	Std. Dev.	Skewness	Excess Kurtosis	Min.	Max.
			α=0.5					
		π=66.7%, ρ=9.6%, σ=30.0%, g_u=9.5%, and g_d=-5.0%						
No Breaks - Comp. Inf.	*Div*	0.18	0.13	0.16	2.46	8.97	0.00	1.64
	g	2.25%	2.25%	0.00%	NA	NA	2.25%	2.25%
	$r_{f,\,1\,day}$	10.83%	10.83%	0.00%	NA	NA	10.83%	10.83%
	S	503.56	423.27	362.95	2.46	9.07	35.63	2812.15
	$Call_{ATM,Short\text{-}T}$	16.03	13.23	11.50	0.79	0.16	0.53	93.12
	$IV_{ATM,Short\text{-}T}$	30.00%	30.00%	0.00%	NA	NA	30.00%	30.00%
Breaks - Comp. Inf.	*Div*	0.18	0.13	0.17	2.56	9.07	0.00	1.66
	g	2.27%	2.25%	4.17%	0.01	-1.19	-4.94%	9.48%
	$r_{f,\,1\,day}$	10.87%	10.85%	1.88%	-0.05	-0.75	9.41%	12.11%
	S	508.52	425.48	388.35	2.27	7.46	47.79	3244.08
	$Call_{ATM,Short\text{-}T}$	22.06	18.65	17.36	1.02	2.51	3.96	101.40
	$IV_{ATM,Short\text{-}T}$	31.23%	31.60%	0.78%	0.31	1.24	30.64%	32.50%
Breaks - Inc. Inf. (Learning)	*Div*	0.18	0.13	0.17	2.56	9.07	0.00	1.66
	g	2.24%	2.22%	2.68%	0.25	-0.35	-1.73%	9.23%
	$r_{f,\,1\,day}$	10.81%	10.80%	0.31%	0.78	-0.38	10.07%	12.01%
	S	507.68	425.47	383.20	2.23	7.28	48.21	3218.93
	$Call_{ATM,Short\text{-}T}$	30.44	28.39	19.24	3.67	19.38	2.28	361.77
	$IV_{ATM,Short\text{-}T}$	36.81%	36.39%	5.30%	5.28	19.80	31.13%	241.62%

Table D1 (continued)
Simulation Summary under Six Alternative Scenarios for Investor's Expectations

Scenario	Variable	Mean	Median	Std. Dev.	Skewness	Excess Kurtosis	Min.	Max.
				α=5.0				
				π=66.7%, ρ=8.9%, σ=5.0%, g_u=8.8%, and g_d=-1.5%				
No Breaks - Comp. Inf.	Div	0.17	0.17	0.03	1.12	1.74	0.10	0.37
	g	3.65%	3.65%	0.00%	NA	NA	3.65%	3.65%
	$r_{f,\,1\,day}$	30.28%	30.28%	0.00%	NA	NA	30.28%	30.28%
	S	216.72	201.33	37.52	1.12	1.74	38.94	321.86
	$Call_{ATM,Short\text{-}T}$	1.19	1.03	0.83	0.52	-0.78	0.01	4.23
	$IV_{ATM,Short\text{-}T}$	5.00%	5.00%	0.00%	NA	NA	5.00%	5.00%
Breaks - Comp. Inf.	Div	0.18	0.17	0.04	1.28	1.92	0.11	0.38
	g	3.66%	3.65%	2.96%	0.00	-1.21	-1.49%	8.78%
	$r_{f,\,1\,day}$	30.35%	30.28%	13.22%	-0.04	-0.95	18.61%	40.27%
	S	218.97	209.28	47.93	1.29	2.66	121.79	554.54
	$Call_{ATM,Short\text{-}T}$	1.69	1.55	0.98	0.76	0.69	0.03	8.70
	$IV_{ATM,Short\text{-}T}$	8.62%	7.79%	0.88%	1.48	3.87	5.76%	14.65%
Breaks - Inc. Inf. (Learning)	Div	0.18	0.17	0.04	1.28	1.92	0.11	0.38
	g	3.64%	3.60%	1.62%	0.08	-0.16	-0.52%	8.33%
	$r_{f,\,1\,day}$	30.21%	29.95%	7.15%	0.04	-0.17	20.97%	39.15%
	S	219.73	207.98	41.98	1.40	2.40	130.84	558.04
	$Call_{ATM,Short\text{-}T}$	10.69	10.40	2.77	2.78	12.46	1.85	52.30
	$IV_{ATM,Short\text{-}T}$	69.12%	68.22%	10.56%	2.45	5.38	19.00%	206.22%
Scenario	Variable	Mean	Median	Std. Dev.	Skewness	Excess Kurtosis	Min.	Max.
				α=5.0				
				π=66.7%, ρ=9.6%, σ=30.0%, g_u=9.5%, and g_d=-5.0%				
No Breaks - Comp. Inf.	Div	0.18	0.13	0.16	2.46	8.97	0.00	1.64
	g	2.25%	2.25%	0.00%	NA	NA	2.25%	2.25%
	$r_{f,\,1\,day}$	22.50%	22.50%	0.00%	NA	NA	22.50%	22.50%
	S	206.85	191.62	144.10	2.46	9.07	22.04	1113.94
	$Call_{ATM,Short\text{-}T}$	6.34	5.26	4.52	0.73	-0.85	0.01	37.11
	$IV_{ATM,Short\text{-}T}$	30.00%	30.00%	0.00%	NA	NA	30.00%	30.00%
Breaks - Comp. Inf.	Div	0.18	0.13	0.17	2.56	9.07	0.00	1.66
	g	2.27%	2.25%	4.17%	0.01	-1.19	-4.94%	9.48%
	$r_{f,\,1\,day}$	22.49%	22.41%	18.80%	-0.07	-0.89	6.79%	35.34%
	S	213.66	201.30	190.36	1.90	5.77	24.36	1660.59
	$Call_{ATM,Short\text{-}T}$	8.95	6.99	8.20	2.94	9.48	1.18	76.88
	$IV_{ATM,Short\text{-}T}$	45.85%	43.49%	2.29%	0.45	2.46	34.94%	47.29%
Breaks - Inc. Inf. (Learning)	Div	0.18	0.13	0.17	2.56	9.07	0.00	1.66
	g	2.24%	2.22%	2.68%	0.25	-0.35	-1.73%	9.23%
	$r_{f,\,1\,day}$	22.66%	22.35%	3.09%	0.80	-0.41	14.01%	35.06%
	S	215.78	211.00	199.09	2.20	7.21	29.15	1688.65
	$Call_{ATM,Short\text{-}T}$	24.09	18.99	21.20	4.30	13.63	2.62	322.85
	$IV_{ATM,Short\text{-}T}$	141.10%	140.70%	23.90%	7.35	9.14	42.40%	346.40%

Table D2

Simulated Properties of the Implied Volatility Surface under Rational Learning

The table contains time series statistics concerning the level, slope, and curvature of the IVS in both the moneyness and maturity dimensions in an economy under breaks and incomplete information with learning. The table shows average simulation outcomes using two parameter set ups. $IV_{ATM,Short\text{-}T}$ is defined in Figure 1. Serial Correlation refers to a Box-Pierce test applied to the first-order Ljung-Box statistic. The ARCH(1) and ARCH(3) statistics are the values of the LM test for ARCH effects using one and three lags, respectively. The percentage of simulations with significant statistics at a 10% size for the associated test statistics are reported in parentheses.

Variable	Mean	Std. Dev.	Skewness	Excess Kurtosis	Serial Correlation	ARCH(1)	ARCH(3)
				α =0.5			
	Panel A: π =66.7%, ρ =8.9%, σ =5.0%, g_u =8.8%, and g_d =-1.5%						
$IV_{ATM,Short\text{-}T}$	13.91%	2.53%	1.73	14.13	67.36	49.36	50.96
					(98.90)	(91.40)	(92.60)
$Slope_{Mon}$	-0.91	0.16	-0.46	5.41	20.49	6.19	10.72
					(79.20)	(40.60)	(45.40)
$Curv_{Mon}$	53.36	25.55	0.37	9.44	26.78	8.65	13.09
					(82.50)	(45.80)	(45.80)
$Slope_{Mat}$	-0.17	0.06	-0.09	4.31	66.18	47.52	49.49
					(98.80)	(91.40)	(89.50)
$Curv_{Mat}$	1.93	0.94	0.15	2.07	56.59	33.03	35.43
					(98.90)	(86.10)	(83.40)
	Panel B: π =66.7%, ρ =9.6%, σ =30.0%, g_u =9.5%, and g_d =-5.0%						
$IV_{ATM,Short\text{-}T}$	36.81%	5.30%	5.28	19.80	57.43	29.67	34.79
					(96.90)	(76.30)	(86.80)
$Slope_{Mon}$	-0.23	0.13	-0.43	8.05	19.90	4.95	9.26
					(78.40)	(38.40)	(41.10)
$Curv_{Mon}$	4.52	3.14	1.42	15.53	23.46	7.68	11.93
					(76.60)	(43.403)	(49.70)
$Slope_{Mat}$	-0.20	0.07	-0.10	7.14	61.83	45.21	42.88
					(95.30)	(89.10)	(80.30)
$Curv_{Mat}$	1.94	0.96	0.49	8.53	46.17	30.51	26.84
					(91.70)	(79.80)	(72.40)
Variable	Mean	Std. Dev.	Skewness	Excess Kurtosis	Serial Correlation	ARCH(1)	ARCH(3)
				α =5.0			
	Panel A: π =66.7%, ρ =8.9%, σ =5.0%, g_u =8.8%, and g_d =-1.5%						
$IV_{ATM,Short\text{-}T}$	69.12%	10.56%	2.45	5.38	55.58	50.47	49.65
					(99.80)	(96.50)	(95.80)
$Slope_{Mon}$	-0.49	0.31	0.24	4.51	30.10	12.95	14.70
					(92.70)	(70.60)	(64.40)
$Curv_{Mon}$	-11.92	4.57	-0.46	4.52	10.08	5.04	6.94
					(67.80)	(41.60)	(35.30)
$Slope_{Mat}$	-1.24	0.38	-0.37	3.02	54.05	46.59	46.40
					(98.50)	(95.10)	(94.10)
$Curv_{Mat}$	12.17	2.53	0.15	5.90	48.90	35.08	36.28
					(98.70)	(92.10)	(90.60)
	Panel B: π =66.7%, ρ =9.6%, σ =30.0%, g_u =9.5%, and g_d =-5.0%						
$IV_{ATM,Short\text{-}T}$	141.10%	23.90%	7.35	9.14	49.04	36.19	41.22
					(96.40)	(89.40)	(87.30)
$Slope_{Mon}$	-0.20	0.29	0.83	6.67	27.99	10.91	13.07
					(77.80)	(62.70)	(62.80)
$Curv_{Mon}$	-4.37	7.34	-0.60	8.43	8.77	4.26	6.19
					(62.70)	(40.10)	(34.80)
$Slope_{Mat}$	-2.69	0.77	-0.34	5.69	49.90	33.18	36.74
					(94.40)	(91.10)	(89.20)
$Curv_{Mat}$	25.97	3.75	0.45	7.74	45.56	30.79	34.12
					(95.10)	(88.30)	(85.90)

Table D3

Cross-Sectional Relationships of IVS Features under Rational Learning

The table contains correlations for the level, slope, and curvature of the IVS in both the moneyness and maturity dimensions in an economy under breaks and incomplete information with learning. The table shows average simulation outcomes using two parameter set ups. $IV_{ATM,Short\text{-}T}$ is defined in Figure 1, while $Slope_{Mon}$, $Curv_{Mon}$, $Slope_{Mat}$, and $Curv_{Mon}$ are defined in Table II. The percentage of simulations with significant statistics at a 10% size for the associated test statistics are reported in parentheses.

Variable	$IV_{ATM,Short\text{-}T}$	$Slope_{Mon}$	$Curv_{Mon}$	$Slope_{Mat}$	$Curv_{Mat}$
			α=0.5		
	Panel A: π=66.7%, ρ=8.9%, σ=5.0%, g_u=8.8%, and g_d=-1.5%				
$IV_{ATM,Short\text{-}T}$	1.00				
	(100.00)				
$Slope_{Mon}$	-0.64	1.00			
	(96.40)	(100.00)			
$Curv_{Mon}$	0.21	-0.83	1.00		
	(68.90)	(96.90)	(100.00)		
$Slope_{Mat}$	-0.95	0.57	0.19	1.00	
	(98.70)	(94.10)	(68.60)	(100.00)	
$Curv_{Mat}$	0.91	-0.51	-0.18	-0.94	1.00
	(98.70)	(93.60)	(61.40)	(98.80)	(100.00)
	Panel B: π=66.7%, ρ=9.6%, σ=30.0%, g_u=9.5%, and g_d=-5.0%				
$IV_{ATM,Short\text{-}T}$	1.00				
	(100.00)				
$Slope_{Mon}$	-0.45	1.00			
	(91.40)	(100.00)			
$Curv_{Mon}$	0.19	-0.49	1.00		
	(65.30)	(94.90)	(100.00)		
$Slope_{Mat}$	-0.40	0.37	0.13	1.00	
	(84.30)	(78.60)	(54.60)	(100.00)	
$Curv_{Mat}$	0.34	-0.09	-0.14	-0.68	1.00
	(78.90)	(55.40)	(59.10)	(86.60)	(100.00)
Variable	$IV_{ATM,Short\text{-}T}$	$Slope_{Mon}$	$Curv_{Mon}$	$Slope_{Mat}$	$Curv_{Mat}$
			α=5.0		
	Panel A: π=66.7%, ρ=8.9%, σ=5.0%, g_u=8.8%, and g_d=-1.5%				
$IV_{ATM,Short\text{-}T}$	1.00				
	(100.00)				
$Slope_{Mon}$	-0.63	1.00			
	(92.80)	(100.00)			
$Curv_{Mon}$	0.60	-0.65	1.00		
	(86.80)	(92.70)	(100.00)		
$Slope_{Mat}$	-0.98	-0.03	0.38	1.00	
	(100.00)	(27.90)	(76.80)	(100.00)	
$Curv_{Mat}$	0.93	0.00	-0.40	-0.95	1.00
	(99.80)	(26.30)	(81.10)	(99.10)	(100.00)
	Panel B: π=66.7%, ρ=9.6%, σ=30.0%, g_u=9.5%, and g_d=-5.0%				
$IV_{ATM,Short\text{-}T}$	1.00				
	(100.00)				
$Slope_{Mon}$	-0.68	1.00			
	(93.50)	(100.00)			
$Curv_{Mon}$	0.54	-0.56	1.00		
	(89.10)	(93.60)	(100.00)		
$Slope_{Mat}$	-0.21	-0.09	0.18	1.00	
	(67.30)	(27.90)	(66.50)	(100.00)	
$Curv_{Mat}$	0.30	0.06	-0.13	-0.23	1.00
	(72.80)	(19.70)	(57.90)	(85.10)	(100.00)

Table E1

Comparing Fitted Deterministic Volatility Functions on Market Data vs. from Simulations from an Economy under Incomplete Information with Rational Learning

The table contains OLS coefficient estimates and fit measures obtained from estimating equation (E1) on average implied volatilities from the U.S. option market vs. simulated option IVs from a Bayesian learning model under alternative calibrations.

	b_0	b_1	b_2	b_3	b_4	b_5	R^2	F Statistic	p-value
	Panel A: π=66.7%, ρ=8.9%, σ=5.0%, g_u=8.8%, and g_d=-1.5%								
α= 0.2	2.70	-4.76	2.21	-0.74	0.20	0.47	0.89	53.84	0.00
α= 0.5	4.12	-7.53	3.52	-0.88	0.13	0.71	0.91	37.70	0.00
α= 5.0	-7.04	14.44	-6.94	-0.32	0.71	-0.68	0.94	71.55	0.00
	Panel B: π=66.7%, ρ=9.6%, σ=30.0%, g_u=9.5%, and g_d=-5.0%								
α= 0.2	2.94	-4.90	2.40	-0.73	0.21	0.48	0.88	49.12	0.00
α= 0.5	4.11	-7.16	3.41	-0.94	0.13	0.72	0.90	36.30	0.00
α= 5.0	-5.54	13.99	-7.03	-0.33	0.72	-0.62	0.93	67.68	0.00
	Market Data								
S&P 500 Options	7.31	-13.55	6.39	0.50	-0.03	0.54	0.85	31.75	0.00
Equity Options	4.60	-8.11	3.92	-0.22	0.05	0.12	0.81	43.61	0.00